

Consumers
Power
Company

General Offices: 212 West Michigan Avenue, Jackson, Michigan 49201 • Area Code 517 788-0550

May 26, 1967

Dr. P. A. Morris, Director
Division of Reactor Licensing
United States Atomic Energy Commission
Washington, D. C. 20545

Re: Docket 50-155

Regulatory Compl File Cy.

Dear Dr. Morris:

Attention: Mr. D. J. Skovholt

Transmitted herewith are three (3) executed and nineteen (19) conformed copies of a request for a change to the Technical Specifications of License DPR-6, Docket No. 50-155, issued to Consumers Power Company on May 1, 1964, for the Big Rock Point Nuclear Plant.

The proposed change (No. 13) will enable Consumers Power Company to insert into the reactor at Big Rock Point six (6) high performance developmental fuel bundles designed to explore the central fuel melting regime. These bundles are an essential part of the "General Electric-Atomic Energy Commission-Euratom Project on UO₂ Fuel Operation With Central Melting in a Large Power Reactor (Contract AT(04-3)-189, PA 50)."

To allow insertion of these bundles, during the present refueling outage at Big Rock Point, requires approval of this request by June 12, 1967. The bundles are presently in the final stages of fabrication at the General Electric Company's facilities in San Jose and can be shipped to meet the above date.

It is recognized that the time interval is extremely short and that we are asking for special handling of this request. To assist you in this matter, we are prepared to come to Washington and spend whatever time is necessary with your staff after they have had an opportunity to review this submittal.

We will appreciate any special attention that you can give to this request. The AEC Reactor Development Division, Euratom and General Electric Company are extremely anxious to get this program under way.



RECORDED

1810

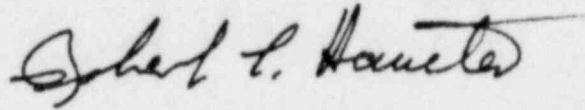
8101190449

Dr. P. A. Morris
May 26, 1967

2

We must apologize for not getting this request submitted earlier; however, the physics, thermal-hydraulics and safety analyses for this design were very time-consuming.

Yours very truly,

A handwritten signature in cursive script, reading "Robert L. Haueter". The signature is written in dark ink and is positioned above the typed name.

Robert L. Haueter
Assistant Electric Production
Superintendent - Nuclear

RLH/dmb
Attach.



CONSUMERS POWER COMPANY

Docket No. 50-155

Regulatory Supply File Case
Request for Authorization of Change in Technical Specifications

License No. DPR-6

I. Changes in Technical Specifications

For the reasons hereinaft set forth, it is requested that the Technical Specifications Appended to Operating License No. DPR-6 issued to Consumers Power Company on May 1, 1964, for the Big Rock Point Nuclear Plant, be changed as follows:

- A. Replace paragraph at beginning of Section 5.1.5 (c) to read as follows:

"The general dimensions and configuration of the types of fuel bundles shall be as shown in Figures 5.2, 5.3, 5.4, 5.5, 5.6 and 8.1 of these specifications. Principal design features shall be essentially as follows:"

- B. Add Figures 5.5 and 5.6 (8 x 8 and 7 x 7 Fuel Drawings).
C. Add a column to the table in Section 5.1.5 (c) as follows:

<u>General</u>	<u>Research and Development</u>	
Geometry, Fuel Rod Array	8 x 8	7 x 7
Rod Pitch, Inches	0.807	0.921
Standard Fuel Rods per Bundle	36	29
Special Fuel Rods per Bundle	28***	20***
Spacers per Bundle	5	5
Material	Zr-2	Zr-2
Standard Rod Tube Wall, Inches	.035	.040
Special Rod Tube Wall, Inches	.035	.040

***Special rods have depleted uranium.

<u>Fuel Rods</u>	<u>Research and Development</u>	
Standard Rod Diameter, Inches	0.570	0.700
Special Rod Diameter, Inches	0.570	0.700
UO ₂ Density, Percent Theoretical	← 94 Pellet → 85 Powder	
Active Fuel Length, Inches	66-67.3	65-66.3
Fill Gas	Helium	Helium"

D. Add a new section as follows:

"5.1.9 Centermelt Test Fuel Bundles

Six fuel bundles may be operated at increased thermal output, up to and including various amounts of center melting of the UO₂. The fuel has been specifically designed for this operation and is permitted to exceed the general core operating limitations of Section 5.2.1 (b) but will be limited to the most conservative of the following values:

<u>Fuel Type</u>	<u>8 x 8</u>	<u>7 x 7</u>
Number of Bundles		
Pellet UO ₂	1	2
Powder UO ₂	1	2
Maximum Steady State Heat Flux, Btu/Hr-Ft ²	500,000	500,000
Maximum Steady State Fuel Rod Power, Kw/Ft	21.8	26.8
Minimum Core Burnout Ratio to Corepower	1.5*	1.5*

Rate of Change of Reactor Power During Reactor Operation:

"Control rod withdrawal will be limited as in Section 5.2.1. In addition, when the centermelt fuel is in the core, the following restriction shall be observed whenever (a) a centermelt fuel bundle is being brought to full power for

*Based upon new Critical Heat Flux Correlation, APED-5286 (see Proposed Change #12).

the first time, or (b) a scram recovery is being made at a time in the xenon transient such that the peak of the axial power distribution is lower in the core than the peak existing at the time of the last shutdown:

When power is between 170 Mwt and 240 Mwt, the rate of power increase will be limited to an average of 1/2 Mwt per minute."

II. Centermelt Fuel Mechanical and Thermal Design

A total of 324 fuel rods will be incorporated into six fuel assemblies for irradiation in the Big Rock Point reactor. Two of the assemblies, comprised of 64 rods each in an 8 x 8 configuration, will be designed for incipient melting of UO_2 at rated power conditions. These assemblies have been designated the intermediate performance fuel and will contain both powder and pellet type fuel. The remaining four assemblies, comprised of 49 rods each in a 7 x 7 configuration, will be designed for definite but moderate melting of the UO_2 at rated power conditions. These assemblies have been designated the advanced performance fuel and contain both powder and pellet type fuel.

The basic fuel bundle design will be similar to that used previously in the high power density research and development program. The ability to remove and replace individual rods during various phases of the irradiation will be of value during the operation of the program. Individual rods can be examined visually, dimensional measurements can be made and selected rods can be shipped to the RML (Radioactive Materials Laboratory) of General Electric Company for destructive examination at various levels of exposure without destroying the integrity of the assembly.

The fuel will be limited to the same critical heat flux ratio as the remainder of the core (MCHFR ≥ 1.5 at an overpower of 1.22). The new critical heat flux correlation, APED-5286, will be used as the basis for the calculations.

Fuel rod size will be such that when operated at a rated surface heat flux of $450,000 \pm 50,000$ Btu/Hr.-Ft² the intermediate performance

fuel will operate with incipient central melting while the advanced performance fuel will operate with definite but moderate central melting.

A. Fuel Bundle Design

Both the advanced performance fuel (0.700" diameter) and the intermediate performance fuel (0.570" diameter) will use the removable rod design used previously in the high power density fuel development program. The 0.700" diameter rods are arranged in a 7 x 7 array. Figure 5.5 describes the fuel assembly in detail. The 0.570" diameter rods are arranged in an 8 x 8 array. Figure 5.6 describes the assembly in detail. Key components of the support structure are as follows:

1. Handle - Completely removable to allow rod removal. Handle has notches to permit visual identification of these bundles after loading into the reactor.
2. Pin - Captures the handle to the support structure.
3. Spacer - Double layer wire, constant pressure spring type. Provides maximum protection against wear of the Zircaloy-2 cladding.
4. Angle - Acts as axial support member of bundle. Provides a means of ^{positioning} ~~position~~ spacers axially. Also minimizes the possibility of damage to rods and spacers during insertion and removal from in-core channel locations.
5. Base - A grid bar arrangement welded to the lower end of each corner angle. The fuel rods rest on the grid.

The support structure is fully capable of supporting the rods when resting on the base and when hung from the handle. However, when resting on a side with a full load of rods, adequate support must be provided for individual rods to prevent damage to the spacers. This will be provided during the shipment of unirradiated bundles, and the method of packing and shipment has been proven to be adequate to prevent damage. Other pertinent design data are shown in Table 1.

The fuel bundles in the fully loaded condition will be of the following approximate weights: (Includes weight of cage.)

1. 0.700 OD Pellet UO₂ Rods - 385 Lb
2. 0.700 OD Powder UO₂ Rods - 358 Lb
3. 0.570 OD Pellet UO₂ Rods - 330 Lb
4. 0.570 OD Powder UO₂ Rods - 309 Lb

B. Fuel Rod Design

1. Intermediate Performance Fuel

There are two intermediate performance fuel assemblies. Each contains 64 rods in an 8 x 8 configuration. Four U-235 enrichments are used in each assembly and one assembly will contain pellet type fuel while the other will contain powder type fuel.

The rods in the assemblies are clad with 0.570" OD x 0.035" wall Zircaloy-2 tubing and contain a compression spring in the plenum region to minimize axial fuel movement during handling and shipping. A depleted UO_2 pellet is to be placed at each end of the active fuel column to minimize temperature effects at the lower end plug and the plenum spring. The UO_2 pellets will be dished to provide a 5% void volume to accommodate the phase change volume expansion of the UO_2 on melting. The UO_2 powder will be compacted to an apparent density of 85% of theoretical. The 15% void volume is adequate to accommodate the volume expansion which will occur in melting for these rods.

Fuel-clad mechanical interaction resulting from differential thermal expansion is considered as one of the largest potential contributors to high cladding strain. In an attempt to minimize this on a gross scale, a rather large cold gap of 0.012" is built into the intermediate performance pellet fuel. At the beginning of life at normal rated power, at least two mils of diametral clearance will be present in the rods. As burnup proceeds, this clearance will decrease to about one mil at 15,000 Mwd/T.

2. Advanced Performance Fuel

There are four advanced performance fuel assemblies, each containing 49 rods in a 7 x 7 configuration. Two of the assemblies will contain UO_2 in the form of sintered pellets and the other two assemblies will contain UO_2 in the form of compactible grade powder.

In the advanced performance fuel, there are three distinct designs. Two differ only in the form of the UO_2 (powder or pellet). The third design is the same except tungsten wafers are placed in the rods at approximately 18" intervals in the axial direction. The purpose of the tungsten wafer is to minimize axial movement of the molten UO_2 during

operation. It is tentatively planned to place tungsten wafers in eight of the high performance rods - four powder rods and four pellet rods.

Tungsten was chosen as the material for the wafers because of its compatibility with UO_2 at high temperatures. The melting point of tungsten is $3370^\circ C$ as compared to $2800^\circ C$ for UO_2 . The thermal conductivity of the tungsten wafer plays an important part in maintaining the adjacent UO_2 below its melting point.

The effect of the tungsten wafers inserted into some of the 0.700" OD 7 x 7 array centermelt bundles has been calculated. The high neutron absorption cross section of tungsten causes a calculated power depression of 2.5% from the maximum value between wafers to the point adjacent to the wafer. The calculation performed with two-dimensional, r-z geometry diffusion theory necessarily assumes symmetric boundary conditions which then assumes that all fuel rods contain wafers. This is not the case, and the actual power depression in the segmented rods will be negligible and lower than the calculated value.

All rods in the advanced performance fuel are clad with 0.700" OD x 0.040" wall Zircaloy-2 tubing and contain a compression spring in the plenum region to minimize axial fuel movement during handling and shipping. The pellet fuel will be fabricated with a 0.100" diameter central hole to accommodate the phase change volume expansion of the UO_2 on melting. The 15% void space is considered sufficient to accommodate the volume expansion on melting in the powder fuel.

Fuel-clad interaction will be minimized in the pellet rods by use of a 0.013" nominal cold gap. At $450,000 \text{ Btu/hr-ft}^2$ heat flux and beginning-of-life conditions, no gross interaction will occur. It is possible, however, that at $15,000 \text{ Mwd/T}$, a very slight degree ^{of interaction} could occur. The combined effects of increased fuel temperature and fission swelling are the cause of this.

3. UO_2 and Cladding Temperature Calculations

Temperatures of the UO_2 and cladding were calculated using the following input information:

UO₂ Thermal Conductivity - The UO₂ thermal conductivities used in this analysis are as follows:

$$\text{Pellet Fuel: } K(T) = \frac{38.24}{402.4 + T} + 6.1256 \times 10^{-13} (T + 273)^3 \quad (1)$$

This equation results in an $\int_0^{2800^\circ \text{C}} KdT = 93 \text{ W/cm}$, and $\int_{500^\circ \text{C}}^{2800^\circ \text{C}} KdT = 62 \text{ W/cm}$.

$$\text{Powder Fuel: } K(T) = \frac{48.39}{1458.6 + T} + 5.2922 \times 10^{-13} (T + 273)^3 \quad (2)$$

This equation results in an $\int_0^{2800^\circ \text{C}} KdT = 63 \text{ W/cm}$, and $\int_{500^\circ \text{C}}^{2800^\circ \text{C}} KdT = 49 \text{ W/cm}$.

The integral KdT for pellets and powder versus temperature is plotted in Figure 1. The pellet integral KdT curves are from Lyons, et al. (1) The powder KdT meets the constraints as suggested by D. H. Coplin in Reference (2), Pages 4-8, and agrees with post-irradiation measurement data points in Reference (1), Figure 7-3. The slope of the powder curves has a K(T) for powder in the range 500° C to 1500° C approximately 25% less than for pellet fuel and, in the range of 1500° C and 2800° C, K(T) is approximately equal to that for pellet fuel.

Specific Heat Generation Required for Melting - The specific heat generation required to cause melting for three conditions is:

	<u>8 x 8 Bundle</u>		<u>7 x 7 Bundle</u>	
	<u>Pellet</u>	<u>Powder</u>	<u>*Pellet</u>	<u>Powder</u>
Beginning of Life	21.4 Kw/Ft	19.1 Kw/Ft	24.2 Kw/Ft	19.4 Kw/Ft
10,000 Mwd/T	20.1 Kw/Ft	18.5 Kw/Ft	22.9 Kw/Ft	19.0 Kw/Ft
20,000 Mwd/T	20.5 Kw/Ft	18.7 Kw/Ft	23.3 Kw/Ft	19.2 Kw/Ft

*Value for $\alpha = 0.164$ where $\alpha = \frac{\text{melt radius}}{\text{pellet radius}}$. $\left(\frac{\text{Center hole radius}}{\text{Pellet radius}} = 0.164 \right)$

Results - The computer results of the calculation of clad and UO₂ temperature and thermal expansion are shown in the following figures. The clad average temperature at any location on the rod is shown as a function of heat flux in Figures 2, 5, 8 and 11. The fuel center line temperature as a function of heat flux is shown in Figures 3, 6, 9 and 12, and the UO₂ melt fraction as a function of heat flux is shown in Figures 4, 7, 10 and 13.

- (1) Lyons, M. F., et al, "UO₂ Thermal Conductivity From Irradiation With Central Melting," GEAP-4624, July 1964.
- (2) Lyons, M. F., et al, "UO₂ Powder and Pellet Thermal Conductivity During Irradiation," GEAP-5100-1, March 1966.

III. Physics Design Analysis

The centermelt bundle designs include four different U-235 enrichments which allow a statistically significant number of fuel rods operating at $450,000 \pm 50,000$ Btu/hr-ft² without exceeding critical heat flux limits. The design goals were the following:

- a. Adherence to the same MCHFR limit as the rest of the core.
- b. Reactivity coefficients which are as negative as possible.
- c. Bundle average exposure capability of 15,000 Mwd/T without bundle modifications (burnable poison in some form).

A. General Features Common to Both Designs

Both the 7 x 7 and the 8 x 8 designs have four enrichments: 4.3, 5.0, 5.6 and 0.22 (depleted) wt percent. The enrichments and placement of the rods were specified such as to provide the maximum number of fuel pins operating at or very close to the desired heat fluxes. The general arrangement of the various enriched rods is shown in Figures 14 and 15.

The number of depleted UO₂ rods was decided from a thermal limit MCHFR consideration, where their low power production effectively increases the allowable power of the remaining enriched fuel rods at the same overall bundle power output. The depleted rods were arrayed in a roughly annular zone inside the corner and side rods above. Then, the highest enrichment rods were placed in a symmetrical arrangement near the center of the bundle. Their enrichment is sufficient to produce rod powers similar to the other outer power producing rods.

The bundles have adequate thermal margins throughout their lifetime based on typical "beginning" and "end of cycle" power shapes. These power shapes are very important to the design and were determined from typical recent operating shapes experienced at Big Rock Point and are the worst expected during normal operation.

Both bundle designs have been enriched to attain approximately 15,000 Mwd/T average (20,000 Mwd/T average for the power producing rods) in a core of the same type. This is the standard method of

specifying fuel bundle exposure capability, and it is possible to "push" any desired bundle or bundles past the specified exposure capability at some expense in core reactivity.

B. Calculated Local Peaking Factors

The calculated local peaking factors for both the 7 x 7 and the 8 x 8 bundles are shown in Figures 14 and 15. The local peaking factors shown are for the new bundle, and the average rod power in each case is 1.0. Because of plutonium production in each of the fuel rods, the peaking factors of the depleted rods will increase with time and, because of normalization, the peaking factors for the enriched higher power producing rods will decrease.

The relative power of the three high enrichment groups decreases with exposure, and the depleted group increases. The fuel will be moved to positions with higher radial power factors as the irradiation proceeds. In this way, the design heat flux for the high enrichment rods can be maintained throughout the exposure lifetime. The bundles are capable of the target heat fluxes at 15,000 Mwd/T average exposure and typical beginning of cycle power shapes without exceeding the critical heat flux limits.

C. Doppler Coefficient

The Doppler coefficient for the 8 x 8 bundle design has been calculated to be $-0.86 \times 10^{-5} \Delta k/k/^{\circ}F$ at $\sim 1000^{\circ} K$. This compares to the standard fuel designs (A, B and C) for Big Rock which have values in the range of -1.0 to $-1.1 \times 10^{-5} \Delta k/k/^{\circ}F$. The 7 x 7 design is about $-0.96 \times 10^{-5} \Delta k/k/^{\circ}F$.

D. Temperature and Void Coefficients

The temperature and void coefficients for the cold center-melt bundles have been calculated. The coefficients are noticeably more positive than standard BRP fuel, as can be seen in the following comparison with BRP "B" reload" fuel presently loaded into the reactor.

	Temperature Coefficient at 25° C		Void Coefficient at 20° C	
	$(\Delta k/k)/^{\circ}\text{C}$		$(\Delta k/k)/\text{Unit Void}$	
	Beginning of Life	End of Life	Beginning of Life	End of Life
"B" Reload With- out Cobalt	$+3.29 \times 10^{-6}$	$+5.5 \times 10^{-5}$	-0.28	-3.8×10^{-2}
Centermelt 8 x 8	$+1.04 \times 10^{-4}$	$+1.8 \times 10^{-4}$	-0.24	$+5.3^* \times 10^{-3}$
Centermelt 7 x 7	$+5.60 \times 10^{-5}$	$+1.7 \times 10^{-4}$	-0.27	-1.3×10^{-2}

*For 0 to 10% voids; the corresponding number for 0 to 20% voids is -6.8×10^{-3} .

The small number of centermelt bundles in the reactor core (six of an 84 total) will produce a very small, if even detectable, effect on overall reactor behavior with temperature and void. The total addition of reactivity due to any possible cold voiding of the two 8 x 8 bundles has been calculated to be 0.0000126 ($\Delta k/k$). The temperature coefficient is negative at the operating temperature. It turns from positive to negative at about 130° C.

E. Burnup Behavior

Although the bundles do not resemble other designs in the core to any great extent, the behavior with lifetime is very similar. The burnup slope for the 7 x 7 bundle is 0.0113 $\Delta k/1000 \text{ Mwd/T}$ and 0.0116 $\Delta k/1000 \text{ Mwd/T}$ for 8 x 8. This compares to the last reload ("C" fuel with cobalt) value of 0.0105 $\Delta k/k/1000 \text{ Mwd/T}$. The beginning reactivities are comparable to the "B" and "C" reload designs, and no special power shape or lifetime behavior problems are expected.

F. Location in Core

The six centermelt test fuel bundles are to be loaded in the core in a dispersed array with a minimum center-to-center distance of 42 cm (16.5"). The fuel bundle plus water gap is a square 7.4" on a side. This restriction means that the closest centermelt bundle spacing will be no closer than two bundles in the x-direction and one in the y-direction. Also, the centermelt bundles will not be placed in the outer row at the periphery of the core. Notches have been placed on the handles of the centermelt bundles to permit visual verification of their location after

they have been loaded into the core. The centermelt fuel is designed to have a bundle power comparable to the adjacent fuel and will not cause excessive flux or power in adjacent fuel bundles.

IV. Experience With Central Melting

This irradiation program can be considered an extension of the high performance UO_2 program which was proposed jointly by the U.S. Atomic Energy Commission and Euratom. This program established the basic feasibility of operation with UO_2 central melting. Forty-three fuel rods were irradiated during the high performance UO_2 program as summarized in Table 2. A brief synopsis of the irradiations is given below. More detailed descriptions of the irradiations are available.^(3,4,5) The correspondence between individual fuel rods and the assemblies in which they were irradiated can be determined from Table 2.

The first three fuel assemblies irradiated contained relatively high-density, solid pellet, fuel rods and were representative of the best design practice at the time. These three assemblies, EPT-6, EPT-8 and EPT-10, were irradiated in consecutive GETR cycles. The third assembly irradiation with EPT-10 was terminated prematurely by indications of a fuel rod failure and all three assemblies showed severe cladding swelling, sufficient to preclude continuation of the irradiations to higher thermal performance levels.

Evaluation of the problem, and especially supplementary capsule irradiation evidence, led to the conclusion that the most probable mechanism for the swelling was the occurrence of a significant UO_2 volume increase accompanying the solid-liquid phase change. The primary evidence for this conclusion was:

-
- (3) Lyons, M. F., et al, "UO₂ Fuel Rod Operation With Gross Central Melting," GEAP-4264, October 1963.
 - (4) Lyons, M. F., et al, "Molten Fuel Rod Operation to High Burnup," GEAP-5100-2.
 - (5) Lyons, M. F., "High Performance UO₂ Program - Irradiation of 0.5 Inch Diameter Vibratory Compacted Powder Fuel Rods at 1.3×10^6 Btu/Hr-Ft² Peak Heat Flux to 10,000 MWD/Te Burnup," GEAP-5100J, September 1966.

1. The correspondence of the maximum swelling zone to the peak heat flux zone at start-up.
2. The correspondence of the threshold thermal performance level for swelling with that required to initiate melting.
3. The apparent increase in swelling with thermal performance level.
4. The distinct axial expansion of the molten UO_2 fuel column in short-length capsule irradiations.

Almost simultaneously with the occurrence of fuel rod clad swelling during these irradiations, new measurements of the UO_2 volume change on melting were reported^(6,7) and they indicated a greater volume increase than previously suspected. Preliminary results suggested a value of 7% which was subsequently refined to 9.6%. Based on these results, it became apparent that higher performance conditions could only be attained by devising a means to accommodate the increased fuel volume.

Two methods were given serious consideration for reducing fuel density to allow for the phase change volume increase:

1. Divide the present through-rod design into capsule length segments and provide axial expansion areas within the molten fuel region, and
2. Use hollow or dished pellets to provide the increased volume.

The use of hollow pellets was finally selected as the most straightforward approach. To evaluate this idea, a special assembly irradiation, designated EPT-COM, was performed with pellets cored with an 85-mil diameter hole, equivalent to ~3% of the fuel volume. The pellets of these four rods were enriched such that a range of performance levels would be obtained. The irradiation of this assembly was performed in two steps:

-
- (6) Christianson, J. A., "Specific Volume of Molten Uranium Dioxide," Paper for American Ceramic Society, 15th Pacific Coast N. W. Regional Meeting, Seattle, Washington, October 1962.
- (7) Christianson, J. A., "Thermal Expansion of UO_2 ," HW-75148, October 1962.

(1) A single short cycle of full power operation followed by examination, and (2) A full cycle of irradiation with normal reactor power cycling. Post-irradiation examination revealed only slight swelling of one rod, Rod 10E, which occurred during the short cycle start-up, with no indications of a ratcheting mechanism during the subsequent continued operation. However, because of the slight swelling of Rod 10E, it was concluded that the free volume provided by the small cored pellets was marginal for a performance level of 1.0×10^6 Btu/hr-ft² and above, and a larger core was provided for the maximum thermal performance irradiation in the sintered pellet series, Assembly EPT-12C.

Assembly EPT-12C, to be irradiated at a nominal performance level of 1.2×10^6 Btu/hr-ft², was provided with sintered pellets cored to an inside diameter of 0.140". This larger core size was selected to provide about 8% (of the UO₂) free volume for the phase change expansion. To protect the rods further, a programmed start-up procedure was introduced in the irradiations. This procedure was formulated in recognition of the significant axial fuel relocation observed in the previously irradiated rods, and the possibility that the relocation could undo the initial benefit of the deliberately included central hole. The objective of the procedure was to prevent any sudden increases in internal volume without allowing time for axial redistribution. The reactor power rise rate was limited to less than 1 Mw (or 3%) per 15-minute time increment and the restriction initiated at a power level below that at which the onset of central melting would be expected. This start-up procedure was specified for all start-ups following a reactor refueling, provided the predicted flux peak location was three inches or more below that existing at the previous shutdown.* In the absence of a refueling resulting in a significant downward flux shift, no restriction on start-up rate was made.

Irradiation of Assembly EPT-12C was successful through the first two reactor cycles to 5300 Mwd/T burnup with no detectable swelling of the rods at performance levels as high as 1.4×10^6 Btu/hr-ft².

*GETR operation results in an axial flux peak shift as control rods are retracted to compensate for reactivity depletion during a reactor cycle. Refueling then results in an abrupt shift of the peak heat flux axial location.

However, on the third cycle start-up, rod swelling and one rod failure occurred. The unexpected result was subsequently traced to an inadvertent 4 Mw (13.3%) step power increase before failure. Two of the rods from the EPT-12C assembly were only slightly swollen and continuation of their irradiation was attempted in two subsequent assemblies, EPT-12C-A and EPT-12C-B. However, both rods experienced pinhole type failures during their initial start-up or very shortly thereafter. No satisfactory explanation for the pinhole failures was obtained, but some connection with the same event that caused the swelling and failure in the other two rods seems inescapable. New cored pellet rods, substantially identical to the EPT-12C rods, were fabricated later and operated satisfactorily to more than twice the EPT-12C assembly burnup in Assembly EX-12A.

Irradiations in the compacted powder UO_2 series were begun with 90.5% dense, vibratory-compacted and swaged rods in Assembly EPW-6/8. Because of the lower as-built density of these rods compared to solid pellets, they were expected to be less susceptible to swelling. Instead, the powder rods showed greater swelling at equivalent thermal performance to the pellets, even with carefully programmed start-ups. This greater swelling was verified in a second assembly irradiation with 90.5% dense rods, EPW-6/8A. However, this same assembly also contained two 88% dense, straight, vibratory-compacted powder rods which demonstrated significantly reduced swelling at higher thermal performance than the two 90.5% dense rods. The effectiveness of reduced initial density in preventing swelling was confirmed in a third assembly containing straight, vibratory-compacted 87% to 88% dense rods, EPW-6/8V. The concept demonstration was then extended to much higher thermal performance levels with the successful irradiation of 83% to 85% dense fuel rods at peak heat fluxes of 1.5×10^6 in a fourth powder assembly, EPW-10/12V.

On the basis of the above experience, the extended irradiation of the maximum thermal performance powder fuel assembly, EPW-12V, was undertaken and carried successfully beyond 10,000 Mwd/T average rod burnup at heat fluxes up to 1.3×10^6 Btu/hr-ft². During the fifth GETR cycle of

irradiation, a fuel rod failure occurred which was subsequently traced to an initial fabrication defect. The failure was a 1/2" long longitudinal split located on the low heat flux side of the rod 4-1/2" from the bottom. It is thought to have resulted from a tubing defect introduced by swaging. Very slight swelling was noted in the rods, which presumably occurred at the time of the initial start-up. Two of the unfailed rods were then transferred to a new assembly with two new cored pellet rods. This assembly, EX-12A, was successfully irradiated for five more GETR reactor cycles at peak heat fluxes up to 1.4×10^6 Btu/hr-ft² which brought the two powder rods to 20,000 Mwd/T average burnup and the two new pellet rods to about 12,000 Mwd/T. Extensive post-irradiation examination of these rods showed no further swelling in the powder rods, none in the pellet rods and no detectable deterioration of any kind. Coupled with the satisfactory irradiation performance, this assembly is considered to have demonstrated the intrinsic feasibility of high burnup operation with gross central melting.

V. Hazards Considerations

A. General Considerations

The centermelt fuel bundles described above and shown in Figures 5.5 and 5.6 are the same basic mechanical design as the Reload "B" and "C" and the Phase I and II R&D bundles. Experience to date with this design has been excellent and there is no reason to expect problems arising out of the design.

B. Normal Operating Considerations

Except for the higher internal temperatures of the UO₂, the thermal design of the centermelt fuel is similar to the fuel currently licensed for use in the Big Rock Point reactor. Table 3 below lists the critical heat flux ratios (CHFR) and coolant properties for the 122% over-power case. This case is for the 8 x 8 assembly for a typically "worst" case of power distribution. The CHFRs are based on the new GE correlation from APED-5286. The 7 x 7 assemblies show similar quality trends but have higher CHFRs. It should be noted that the minimum critical heat flux ratio (MCHFR) for this typically "worst" power distribution is within the current Big Rock Point license limit for MCHFR. This has been achieved

by including very low power fuel rods in the bundle with the high power centermelt rods. This combination yields essentially the same node-by-node coolant quality profiles as in the current fuel licensed for the Big Rock Point reactor.

TABLE 3
Heat Flux and Coolant Property Data
for a Typically "Worst" Power Distribution
at 122% Overpower (8 x 8 Assembly)

Node	*Axial Power Factor	Surface Heat Flux, Btu/Hr-Ft ²	Surface Temp °F	CHFR	Coolant Quality
1	0.391	0.1513 + 006	590.6	5.8	0.
2	0.510	0.1978 + 006	591.2	4.5	0.
3	0.630	0.2443 + 006	591.7	3.6	0.
4	0.740	0.2870 + 006	592.1	3.1	0.
5	0.830	0.3219 + 006	592.4	2.7	0.
6	0.910	0.3529 + 006	592.6	2.5	0.
7	0.970	0.3762 + 006	592.8	2.3	0.002
8	1.030	0.3995 + 006	592.9	2.2	0.010
9	1.060	0.4111 + 006	593.0	2.1	0.019
10	1.090	0.4228 + 006	593.1	2.1	0.027
11	1.100	0.4266 + 006	593.1	2.1	0.036
12	1.130	0.4383 + 006	593.2	2.0	0.046
13	1.180	0.4577 + 006	593.3	1.9	0.055
14	1.270	0.4926 + 006	593.5	1.8	0.066
15	1.380	0.5352 + 006	593.8	1.6	0.077
16	1.400	0.5430 + 006	593.8	1.5**	0.088
17	1.310	0.5081 + 006	593.6	1.6	0.099
18	1.180	0.4577 + 006	593.3	1.7	0.109
19	1.040	0.4034 + 006	593.0	1.9	0.117
20	0.850	0.3297 + 006	592.4	2.2	0.124

*Mass Flow Rate = 0.75×10^6 Lbm/Hr-Ft², Radial Power Factor = 1.16,
Local Power Factor = 1.60

**Minimum Critical Heat Flux Ratio (MCHFR)

C. Accident Analyses

1. Loss-of-Coolant Accident

The implications of the higher power rating of the center-melt fuel rods on emergency cooling system performance as described in Big Rock Point license change No. 8 have been appraised. Two aspects of the higher power rating are considered to be of significance:

- a. The increased stored energy in the centermelt fuel resulting from its higher average operating temperature level.
- b. The larger decay heat generation rate; this, of course, is directly proportional to the higher design power level of the center-melt fuel.

It is particularly significant to note that this change request relates to the introduction of a maximum of six experimental assemblies into the Big Rock Point core. Each of these assemblies is constituted partially of higher rating (centermelt) rods, the balance being of a low rating such that overall the fuel bundle generates a power level comparable to that of a standard bundle. Consequently, the decay heat generation rates for the complete centermelt assemblies are comparable to the maximum levels computed for previous fuel assembly designs for the Big Rock Point core, even though the individual centermelt (high heat flux) rods within the core will have proportionately higher decay power levels. In view of this planned maximum core loading of six centermelt bundles under the present program, the centermelt rods will constitute only about 2% of the total number of rods making up the core.

Analysis of the effect of increased stored energy in the centermelt rods on fuel temperature following a major system rupture, as discussed in Big Rock Point license change No. 8, indicates the following: As a consequence of the duration of the postulated blowdown (>4 seconds) and of the high heat transfer rates expected in the core during this process, these centermelt fuel rod temperatures will be reduced to a level characteristic of the ensuing decay power generation and are thus virtually independent of the initial stored energy content. This aspect of the center-melt fuel design is therefore not expected to influence the consequences of a loss-of-coolant accident.

The effect of the increased decay heat level of individual rods within an assembly containing a proportionate number of underrated rods, such that on the average the fuel bundle decay power is unchanged, is in this case minimal and is found to be within the limits of accuracy of the temperature measurements ($\pm 100^\circ$ F at 2000° F) carried out by the General Electric Company in the various spray cooling test programs conducted in support of BWR safety analyses. Undoubtedly the general effect is one of increased temperatures as necessary to dissipate the increased decay heat flux. However, at the higher temperature levels ($>2000^\circ$ F) of prime interest from the viewpoint of zirconium behavior in water reactor accidents, a 200° F increase in temperature not only radically increases the evaporative cooling rate for the rods but also increases the radiative heat transfer by 25% or more. This trend is well illustrated by Figure ~~16~~³⁰, attached.

As a result of the proportionate number of low rating rods also present and dispersed relatively uniformly through the bundle, the net effect will be somewhat less than that implied by Figure 16. Furthermore, as this effect will only apply to some 2% of the rods in the core, its significance on the degree of zirconium water reaction and, indeed, on the whole course of the loss-of-coolant accident is minimal and is within the uncertainty margin of available computational techniques.

2. Control Rod Drop Accidents

The Big Rock Point reactor operates with one specified rod withdrawal pattern. The rods are grouped in banks of two or more; all the rods in a bank are withdrawn together, with a procedural limit of one notch between any two rods in a bank. This sequencing prevents large rod worths; however, an operator error or series of errors can result in larger worths.

The possible rod drop situations and rod strengths when the core is critical and at hot standby are:

Case 1: In-sequence potential of .008 Δk for drop from full-in position to drive position.

Case 2: In-sequence potential of .021 Δk for drop from full-in to full-out.

Case 3: Out-of-sequence potential of less than $.021 \Delta k$ for drop from full-in to full-out.

Case 4: Maximum theoretical worst case of about $.045 \Delta k$.

Case 1 requires the following equipment malfunctions and operator error:

- a. Rod becomes uncoupled from drive.
- b. Drive is withdrawn (in-sequence), but blade hangs up temporarily. Operator does not notice that blade is not following.
- c. Rod then unexpectedly releases and drops from full-in to position of the drive due to gravity.

Case 2 requires an additional operator error of withdrawing the drive completely rather than concurrent with the bank.

Case 3 consequences are less than those for Case 2.

Case 4 is considered hypothetical, as it requires still further compounding of unrelated errors beyond those enumerated above.

The analyses are performed for the hot standby (HSB) condition, i.e., power at neutron source level and normal water level in the vessel. The hot standby rather than cold case is analyzed because:

- a. The rod strengths in the cold condition for the same potential rod drop situations are no greater than in the hot standby condition.
- b. According to our calculations, primary system integrity is more vulnerable when there is a free surface of the possible water-hammer and subsequent vessel movement. This situation exists so long as the reactor is critical only when the vessel is at a temperature safely above the minimum ductility temperature. Maintenance of this safety margin allows a strain to rupture, of at least 13%. Big Rock Point operating procedures provide this margin.

The zero power initial condition accidents are more severe than full power accidents because:

- a. The comparable rod strength is less at full power; e.g., the worth for Case 2 is .0095.
- b. The core void gives the moderator system more compliance, thus the water-hammer situation is not as severe.

To prevent a large amount of centermelt fuel from being in the peak neutron flux during a reactivity accident, the six centermelt bundles are to be loaded in the core in a dispersed array with a minimum center-to-center distance of 42 cm. This restriction means that the closest centermelt bundle spacing will be no closer than two bundles in the x-direction and one in the y-direction.

- a. Analytical Methods and Results

The latest analytical tools and methods were employed throughout the present analysis. A brief description of the methods and changes from the "C" core analysis follows:

- i. Neutron Kinetics Methods - The kinetics analysis analytical model was essentially unchanged from that used in the submittal for change No. 10. It should, however, be pointed out that the calculations for change No. 10 were among the first done using this kinetics analysis analytical model. Since that time, the input parameters have been refined. The results of this analysis differ from those submitted earlier in change request No. 10. These refinements of input data are discussed later on in this submittal.

- (a) To incorporate reactor spatial effects into the Doppler feedback to the kinetics calculation, a space-time kinetics analysis is synthesized by a marching calculation. Initial neutron flux distribution associated with accidental reactivity addition is first determined utilizing a three-group, steady state diffusion calculation. A core averaged Doppler spatial weighting factor is estimated from the flux distributions and utilized in the point kinetics equation to generate a small increment of power. In this case, the kinetics calculation represents the average reactor condition.

This increment of power, expressed as a fuel temperature change, is then spatially distributed across the core according

to initial flux distributions. New spatially distributed cross sections are computed, reflecting the Doppler effect due to the added temperature, and another diffusion calculation is made. Comparison of the eigenvalue change in this calculation to the eigenvalue change resulting from a uniformly distributed temperature increment provides an accurate estimate of the Doppler weighting factor appropriate for the next kinetics calculational step. Utilizing this procedure, the calculation is marched through to the termination of the excursion. The space-time dependent calculation includes the inherent power flattening as fuel is heated in the zone of the dropped control blade.

(b) For excursions commencing at zero power and having relatively large reactivity insertions ($.025 \Delta k$ or greater) at gravity rod drop rates, the Doppler effect turns the primary power burst over before all the reactivity has been inserted. This additional reactivity will cause another prompt power burst if there is no negative reactivity immediately available in the system. The scram is assumed not to actuate until 200 milliseconds after the overpower condition is reached, so it can do no better than terminate a second burst, not prevent it.

For the centermelt core all reactivity insertions greater than about $.02 \Delta k$ produce some material of an energy above 425 cal/g, the prompt rupture threshold. This material will disperse in surrounding water and create a rapid steam explosion. Dispersal of the highly enriched centermelt fuel into the moderator is a considerable negative reactivity effect. For example, complete homogenization creates a reduction of approximately 16% in k_{∞} of a bundle. Proper volume and importance weighting of such an occurrence would indicate the whole core effect, and it could be as much as a negative $.02 \Delta k$. Removal of moderator and fuel material or just moderator from the core with a steam explosion is also a considerable negative reactivity effect. The effect of these reactivity changes is not only one of reduced reactor power but also a spatial shift of the peak neutron flux away from the affected area. Now, even in the end of spectrum reactivity insertion, $.045 \Delta k$, the great majority of fuel reaching high energy is located in the centermelt bundle adjacent to the

dropped rod. Thus, the spatial neutron shift to a lower reactivity region at the greatly reduced core power does not significantly increase the amount of fuel containing prompt rupture energy.

Considering that dispersal, steam explosion and flux spatial shift occur in several milliseconds, while a second prompt power burst would not occur until tens of milliseconds after the first burst, the second power burst is prevented or at least severely restricted. It is for this reason that the kinetics analysis for accidents producing a steam explosion does not include the calculated integrated energy found in a second power burst.

(c) The excursions are assumed to be adiabatic with only the Doppler effect supplying prompt reactivity feedback to terminate the primary power burst. In particular, no negative feedback from prompt moderator heating is assumed. The magnitude of the reactivity effect due to Doppler broadening in the calculation has a nominal conservative bias of about 20% in predicted reactivity decrement. This inferred bias is due to a number of factors. Experimental data on UO_2 fuel against which the design model is compared is that of Pettus¹ and Hellstrand². This comparison shows an average conservative bias of the design model on the order of 5% to 10%. In addition, there is about a 3% conservatism introduced through the assumption of a constant radial fuel temperature³. The contribution of Pu-240 to the Doppler reactivity has not been assumed. This effect will increase the decrement by 10% to 15% throughout most of the reactor life.

The temperature dependence of the Doppler coefficient used in all of the analyses is based on the inverse square-root of temperature form. Experimental data for oxide fuel are fit more precisely by this form in both differential measurements^{1,2} and integral measurements of lattice parameters⁴. Analysis of SPERT oxide core excursions⁵, utilizing this Doppler model and the space-time kinetics calculation discussed above, have shown the calculations to give excellent agreement on both the measured peak excursion power and total energy release.

(d) The zero power accident has historically been initiated at a power level of 10^{-6} of rated. As the accident severity decreases monotonically with increasing initial power level in the zero power range further investigation has been undertaken.

Our analysis indicates a free surface is necessary if a water-hammer-activated vessel movement is to occur. Normal start-up procedure insures that whenever the reactor vessel has a free water surface, i.e., it is not full of water, the core power is at least 10% of rated. However, it is conceivable that a lower power could be obtained with a forced shutdown, at which time the isolation valves are closed, momentarily preventing the steam drum to backfill into the pressure vessel. It is this improbable situation that is postulated to embody both a free surface and a zero power condition. However, the power level must be at least as great as the neutron source level. There are two 8,000 curie $\frac{50-B_0}{124}e$ sources in the Big Rock Point Plant. Conservatively assuming the plant has been previously shut down for one source half-life, six months, and considering their location for effective neutron production to the core, the total source level is 3,000 curies. Using this value, the relationship between core effective multiplication constant, k_{eff} , and power is calculated and presented on Figure 16. It is seen that for a power of 10^{-6} the core is .002 Δk subcritical. Using the various combinations described by the line on Figure 16, it was determined that an initial power of 2×10^{-6} times rated and .001 Δk subcritical yielded the most severe results for insertion of .021 Δk or less. For larger insertions, this effect was of little consequence, and the historical values of 10^{-6} rated power and just critical were used. This work also indicates the conservativeness of the historical cold accident initial conditions of 10^{-8} rated power and just critical.

(e) For the rod dropping from full-in with gravity the power burst occurs in the vicinity of 50% withdrawn, depending upon the reactivity worth of the rod. This gives a relatively large axial power peaking. For a rod ejection, the rod will be withdrawn completely when the power burst occurs, thus giving a normal cosine axial power shape.

In the "C" core analysis, the peaked axial shape was used in the ejection calculation; in this analysis the cosine shape is used. In addition, the rod drop analysis was performed on a radially central control rod due to the limitations of our models. This is conservative in that a greater total peaking is obtained than for an off-center reactivity addition in a small leakage controlled core such as Big Rock Point. As it was not necessary to model the axial effects dynamically in the ejection situation, the actual situation of an off-center rod was analyzed. An off-center rod should always be analyzed as they are of highest worth at Big Rock Point, and it is improbable that a centermelt bundle will be placed in the center of the core.

ii. Results of Kinetics Analysis - The peak energy density results of the kinetics analysis are shown on Figure 17. As was explained in the methods descriptions, when the energy density exceeds the prompt rupture threshold of 425 cal/g, the power burst is terminated before any secondary prompt reactivity burst appears. This explains why the slopes of the free fall curves are reduced at prompt rupture energies. The "C" core and centermelt core results are essentially separated by the peak bundle local power factors in the two cores, that is the centermelt bundle of highest specific power is assumed to be adjacent to the dropped control rod.

The peak energy density of low reactivity ejections is not as great as would be expected relative to the corresponding free fall drop. This is explained in the methods discussion by more realistic analysis in the ejection cases.

As indicated previously, the primary difference between the two cores is the local peaking distribution. This is vividly demonstrated on Figure 18, the peaking distribution at peak power as a result of a .025 Δk rod drop.

The final energy distribution is illustrated in Figure 19. Prompt rupture is indicated by an energy density of 425 cal/g and the melting range by 220 cal/g to 280 cal/g. From Figure 19, it is seen that the mass of molten fuel is greater in the "C" core for the same

reactivity addition; however, the amount of fuel undergoing prompt rupture is less. The reason for more molten mass, as explained in the methods discussion, is due to the shutdown provided by the steam explosion in the centermelt core. As far as steam explosion effects are concerned, the primary component is the amount of fuel promptly dispersed into the moderator.

iii. Heat Transfer Methods - The heat transfer mechanism can be visualized in the following steps:

- (a) Loss of clad integrity.
- (b) Fuel dispersal.
- (c) Vapor pressure adjustment to ambient.
- (d) Particle heat dissipation.

There is little time lapse between each of the above occurrences for a particular fuel rod. The specific character of the process depends on the accident parameters of peak energy density, reactor period and fuel particle size.

(a) Loss of Clad Integrity - The shape of a power burst can be reasonably represented by a Gaussian distribution. The total energy density deposited in the fuel is simply proportional to the time integral of the Gaussian. From the kinetics calculations, the shape of the Gaussian, defined by its standard deviation, can be found for each reactivity addition. The standard deviations for the Big Rock Point rod drop accidents vary between 5 and 8 milliseconds corresponding to the .045 Δk insertions, respectively. With this knowledge and the assumption that prompt rupture occurs when the fuel enthalpy reaches 425 cal/g, the relative time of prompt failures can be found. For final enthalpies less than 425 cal/g, the modes of failure vary from fuel vapor pressure exceeding hot cladding strength to cladding meltdown. Cladding failure is assumed not to occur for final energies less than 150 cal/g. The relationship used in subsequent calculations is shown on Figure 20. In the prompt rupture domain it primarily represents the short period, large insertion accident which means it is conservative for the lesser accidents.

(b) Fuel Dispersal - When the clad is breached by internal vapor pressure, the fuel is assumed to disperse instantaneously

into the surrounding water in the form of small spherical particles. The available transient data⁶ with rod-type UO_2 fuel, powder or pellet, indicates a distribution of particle sizes from a few mils in diameter to the original fuel diameter. As the data has been taken with fuel lengths from .5" to 5", an axial power distribution would not seem to be important. Irrespective of the reasons for the wide particle distribution, it has been shown to occur; thus, an effective particle size, properly reflecting the surface area to mass ratio, should give the correct heat transfer calculational results.

(c) Vapor Particle Heat Transfer - When the hot fuel is exposed to a lower pressure atmosphere, 1000 psi, the tendency will be to vaporize more until its vapor pressure is in equilibrium with its temperature. This will be nearly an instantaneous operation. However, particle quenching by the water will also commence, and this energy transfer is taken into account by the particle time constant. It is thought realistic to instantaneously add a quantity of energy to the water to account for the extremely small vapor particles. Somewhat arbitrarily 30 cal/g is added, immediately bringing the UO_2 to a level of 395 cal/g which has a relatively low vapor pressure.

(d) Particle Heat Dissipation - As explained in the discussion of fuel failure, various fuel pins reach prompt breach energies at various times on the back side of the power burst. If the power burst has not terminated, there will continue to be fissioning in the dispersed fuel. As discussed previously, this fissioning will be at a lower rate relative to the core average than when the pins were intact due to the neutron flux shift. The heat generated in this manner must be dissipated at about the same rate as generated because of the proximity of the fuel temperature to the vaporization range. Conservatively assuming no flux shift occurs, this heat transfer rate is taken as the lower limit for this analysis. Now the power burst is an exponential decaying function, so an e-folding time constant, τ , is used to describe the heat transfer rate. Figure 21 shows the time constant used to be a minimum of 15 ms in the high energy density range. As this particular heat transfer analysis

does not apply to any fuel at energy density less than prompt failure, 425 cal/g, a constant value of 100 ms was used for the time constant of particles that were not dispersed during the power burst.

The upper limit on heat transfer rate is the particle property-dependent internal conduction. This rate calculation uses an infinite particle surface heat transfer coefficient. The fission generation should also be included in this upper limit; however, its time constant is large compared to the conduction constants so the effect is small. These time constants are shown on Figure 22 for the various particle sizes. The minimum curve corresponds to a UO_2 heat capacity of .08 cal/g °C. However, the latest data⁷ indicates that the heat capacity in the temperature range just below melting is about .15 cal/g °C.

Now many materials similar to UO_2 have essentially the same heat capacity in the molten state as at temperatures just below melting. With this assumption for UO_2 , heat transfer time constants are larger, as indicated on Figure 22. In addition the ANL-TREAT calculated time constants used in the previous "C" core analysis are shown as well as a radiation controlled heat transfer rate. For conservatism, this analysis used the conduction relationship calculated with the lesser heat capacity. The question of particle size distribution at the time of dispersal is not easily answered. It is believed the TREAT tests are the most representative of BWR transients that exist from the standpoint of fuel failure mechanisms and particle sizes. Argonne National Laboratory has published a reasonable correlation between final mean diameter and peak enthalpy for these tests⁶. This correlation indicates that the mean diameter for fuels undergoing prompt rupture is about 20 mils. From Figure 22, this diameter gives a time constant of 4 ms. which is used in Figure 21. The time constants for less than prompt rupture energy are also direct functions of the TREAT data.

There are now two sets of heat transfer rates with which to bound the problem, fission energy generation and conduction limited. As mentioned above, both are somewhat conservative as in the face of uncertainty the time constants are decreased.

iv. Thermodynamic-Hydrodynamic Analysis - There are many input parameters to this calculation that are not well understood. For this reason, it is realistic to show the effect of varying these parameters rather than choosing a particular value. This analysis uses extreme values of the two most important time variant inputs, the flow path of the water slug and the energy deposition into the water.

The energy deposition extremes were discussed previously and are identified by internal conduction limited and fission heat generation limited. A third set of values corresponding to the TREAT transient powder data is also used. A mathematical expression derived from the basic differential equation describes the flow path in terms of volume velocity and kinetic energy; it is called restraint. The minimum restraint to flow is defined as a cylindrical column of water having a cross-sectional area equal to that of the vessel. The maximum restraint is defined as a cylindrical column with a cross section equal to that of one bundle, e.g., the centermelt bundle adjacent to the dropped rod. From theoretical considerations, the flow path should be somewhat conical in nature. Thus, a best guess flow restraint is chosen to physically represent a two-dimensional flow path with dimensions in between the two extreme one-dimensional situations.

The two important primary system rupture modes are vessel vertical movement with subsequent shearing of pipes and vessel overstrain. The limit of allowable movement on the steam risers and coolant recirculation lines is about 6". However, the limiting case is an allowable 1.5" on the small core spray line. The limit on the Big Rock Point vessel ductility after 40 years of operation has been determined to be 13% strain.

The calculational results are shown on Figures 23 and 24. Some general trends can be noted:

(a) The higher the restraint, the greater the steam pressure and thus the vessel strain. With the high restraint value, there is no vessel vertical movement.

(b) The lower the restraint, the greater the vessel movement. There is no strain with the minimum restraint.

(c) There is no threat to primary system rupture unless there is a significant amount of fuel in the prompt rupture domain greater than 425 cal/g.

D. Conclusions

Based upon the above analyses and comparisons of a whole core of "C" fuel and a core of "C" fuel containing six centermelt bundles, the following conclusions may be drawn:

1. The mechanical design of the centermelt fuel bundles is a well-proven concept and no problems should be expected based on the good experience with the design to date.

2. The total power generated in each centermelt fuel bundle matches the power generated by currently licensed fuel for the Big Rock Point reactor. This yields equivalent coolant quality profiles and MCHFRs. Consequently, currently licensed MCHFR limits can be readily met.

3. The addition of a maximum of six centermelt fuel bundles with their relatively small number of higher performance fuel rods does not significantly change the loss-of-coolant accident. The high performance centermelt rods will constitute only about 2% of the total number of rods in the reactor core. Even though the centermelt rods would have an increased decay heat level, the higher rod temperatures radically increase their evaporative cooling rate and also increase their radiative heat transfer by 25% or more. Consequently, the effect of the six centermelt fuel bundles on the loss-of-coolant accident is minimal.

4. The rod drop accident is not expected to cause a break of the primary system for the following reasons:

a. The maximum control rod worth obtainable with one procedural error is about .021 Δk . The theoretical maximum rod worth is about .045 Δk . The attainment of this high a rod worth requires several procedural errors in succession. Because only one control rod withdrawal pattern is used at any one time, we consider this contingency as being incredible.

b. Considering reactivity accidents, the primary difference between the "C" core and the centermelt core is the increased local peaking in the latter. The free fall drop of the .021 Δk rod mentioned above yields peak energy densities of about 330 cal/g and 450 cal/g in the "C" and centermelt cores, respectively. Neither of these values represents a severe threat to the integrity of the primary system.

c. Because of the restriction on location of the centermelt bundles, all of the elevated temperature fuel is located in the centermelt bundle assumed to be adjacent to the dropped control rod.

d. No threat to primary system integrity was calculated to exist for accidents not having a significant amount of fuel in the prompt rupture domain (>425 cal/g).

e. Using extreme energy addition rates and thermal to mechanical conversion efficiency, the calculated vessel strain as a result of a free fall rod drop of maximum worth in the centermelt core did not reach the vessel ductility limit.

f. Under the most extreme set of assumptions, the calculated vessel vertical movement as a result of a free fall rod drop of maximum worth in the centermelt core would exceed the possible primary system rupture limit. It should be pointed out, however, that these analyses were all done ignoring the resistance to vessel vertical movement provided by the vessel support system. Considering this and the other conservatisms in the calculation, along with the extremely low probabilities of the contingent string of events, it is very unlikely that the primary system would be breached, even under the most extreme set of assumptions analyzed.

Based on the above considerations, we have concluded that the use of centermelt fuel in the Big Rock Point reactor does not present a significant change in the hazards considerations described or implicit in the Final Hazards Summary Report.

CONSUMERS POWER COMPANY

By *H. K. Wall*
Vice President

Date: May 26, 1967

Sworn and subscribed to before me this 26th day of May 1967.

Grace R. Warner
Notary Public, Jackson County, Michigan
My Commission Expires February 16, 1968

TABLE 1

CENTERMELT FUEL DESIGN DETAILS AND OPERATING CONDITIONS

<u>Fuel Assembly</u>	<u>UO₂ Fuel</u>			<u>Number of Rods</u>	<u>Cladding</u>			
	<u>Type</u>	<u>TD</u>	<u>U-235</u>		<u>Type</u>	<u>Outside Diameter (Inches)</u>	<u>Wall Thickness (Inches)</u>	<u>Condition</u>
<u>Group A</u>								
D-50 (8 x 8 Lattice)	Pellet	95	4.3	12	Zirc-2 (Tube Reduction Process)	0.570	0.035	Cold Worked and Stress Relieved
	Pellet	95	5.0	16				
	Pellet	95	5.6	8				
	Powder	85	0.22	28				
D-51 (8 x 8 Lattice)	Powder	85	4.3	12	Zirc-2 (Tube Reduction Process)	0.570	0.035	Cold Worked and Stress Relieved
	Powder	85	5.0	16				
	Powder	85	5.6	8				
	Powder	85	0.22	28				
<u>Group B</u>								
D-52 and D-53 (7 x 7 Lattice)	Pellet	95	4.3	12	Zirc-2 (Tube Reduction Process)	0.700	0.040	Cold Worked and Stress Relieved
	*Pellet	95	5.0	12				
	Pellet	95	5.6	5				
	Powder	85	0.22	20				
D-54 and D-55 (7 x 7 Lattice)	Powder	85	4.3	12	Zirc-2 (Tube Reduction Process)	0.700	0.040	Cold Worked and Stress Relieved
	*Powder	85	5.0	12				
	Powder	85	5.6	5				
	Powder	85	0.22	20				

*Four rods of pellet fuel and four rods of powder fuel of this enrichment (eight rod total) will be segmented by tungsten wafers into lengths of about 17".



TABLE 1

CENTERMELT FUEL DESIGN DETAILS AND OPERATING CONDITIONS (Contd)

<u>UO₂ Fuel</u>	<u>Fuel Rod</u>	Design Burnup (Mwd/TU)	<u>Design Heat Flux</u>		<u>Fuel Rod Power</u>	
			<u>Normal</u> (Btu/Hr-Ft ²)	<u>Overpower</u> (Btu/Hr-Ft ²)	<u>Normal</u> Kw/Ft	<u>Overpower</u> Kw/Ft
<u>Group A (8 x 8)</u>						
Cold Press and Sinter	Standard Dished 5%	20,000	450,000	610,000	19.65	26.6
			+50,000		+2.18	
Dynapak	Vibratory Compaction	20,000	450,000	610,000	19.65	26.6
			+50,000		+2.18	
<u>Group B (7 x 7)</u>						
Cold Press and Sinter	Standard 0.100" Central Hole	20,000	450,000	610,000	24.15	32.8
			+50,000		+2.68	
Dynapak	Vibratory Compaction	20,000	450,000	610,000	24.15	32.8
			+50,000		+2.68	

TABLE 2. Fabrication and Irradiation Data

Assembly No. and Fuel Type	Rod Number	GETR Cycle	Pre - Irradiation Cladding Diameter (Inches)		Fuel Pellet-Clad Diametral Gap (mils)	Fuel Rod Length (Inches)	Fuel Column Length (Inches)	Max. Surface Heat Flux Btu/h-ft ²
			Outside	Inside				
EPT-6 Solid Pellets	6A	33	0.5647-0.5653	0.5058-0.5064	5.5	39.018	33-3/4	630,000
	6B		0.5642-0.5659	0.5060-0.5067	5.8	39.008	34-5/16	665,000
	6C		0.5611-0.5638	0.5064-0.5068	6.1	39.006	34-1/4	675,000
	6D		0.5642-0.5654	0.5051-0.5056	5.9	39.004	34-3/16	732,000
EPT-8 Solid Pellets	8A	33	0.5642-0.5652	0.5092-0.5106	6.4	39.014	34-1/4	950,000
	8B		0.5642-0.5668	0.5082-0.5091	5.1	39.020	34-9/32	920,000
	8C		0.5645-0.5663	0.5091-0.5100	6.0	39.031	34-3/16	780,000
	8D		0.5635-0.5648	0.5092-0.5100	6.1	39.032	34-1/4	915,000
EPT-10 Solid Pellets	10A	35	0.5671-0.5688	0.5093-0.5101	5.7	39.033	31-1/4	1,030,000
	10B		0.5675-0.5685	0.5094-0.5107	6.0	39.012	31-3/8	1,040,000
	10C		0.5663-0.5680	0.5100-0.5104	6.2	39.026	31-5/16	1,140,000
	10D		0.5668-0.5690	0.5097-0.5107	6.2	39.025	31-1/4	1,140,000
EPT-COM Small Cored Pellets	6E	37, 39	0.5647-0.5660	0.5046-0.5055	4.5	38.965	33-3/4	605,000
	8E		0.5635-0.5657	0.5092-0.5100	6.1	38.960	34	905,000
	10E		0.5679-0.5688	0.5098-0.5109	6.3	38.990	31-1/8	1,000,000
	12E		0.5685-0.5690	0.5108-0.5110	9.0	38.990	29-1/2	1,148,000
EPT-12C Large Cored Pellets	12AC	41, 42, 45	0.5620-0.5630	0.5001-0.5006	4.8	39.032	29-1/2	1,440,000
	12BC		0.5620-0.5630	0.5001-0.5018	5.4	39.036	29-1/2	1,360,000
	12CC		0.5610-0.5620	0.5000-0.5009	5.0	39.035	29-1/2	1,210,000
	12DC		0.5610-0.5630	0.5002-0.5009	5.0	39.045	29-3/4	1,250,000
EPT-12CA Large Cored Pellets	12BC	47	0.5620-0.5640	-	-	39.056	-	1,137,000
	12CC		0.5610-0.5630	-	-	39.069	-	1,107,000
	12GC		0.5610-0.5620	-	-	39.054	29-11/16	1,098,000
	12HC		0.5590-0.5605	-	-	39.051	29-5/8	960,000
EPT-12CB Large Cored Pellets	12CC	52	0.5600-0.5640	-	-	39.069	-	1,177,000
	12FC		-	-	-	-	29-11/16	1,230,000
	12HC		0.5590-0.5605	-	-	39.079	-	1,233,000
	12GC		0.5600-0.5630	-	-	39.062	-	1,061,000



TABLE 2. (Continued)

Assembly No. and Fuel Type	Rod Number	GETR Cycle	Pre - Irradiation Cladding Diameter (Inches)		Powder Rod Densities	Fuel Rod Length (Inches)	Fuel Column Length (Inches)	Max. Surface Heat Flux Btu/h-ft ²
			Outside	Inside				
EPW-6/8 Vipac and Swaged Powder	6AA1	40	0.5654-0.5671	-	91%	39.034	34-1/8	531,000
	6AA4		0.5671-0.5682	-		38.924	34-1/8	536,000
	8AA2		0.5670-0.5695	-		39.067	34-1/8	721,000
	8AA4		0.5673-0.5695	-		39.992	34-1/8	615,000
EPW-6/8A Vipac and Swaged Powder 90%TD Vipac Powder	6AA1	40	0.565 -0.567	-	91%	39.026	-	642,000
	8AA4		0.5655-0.569	-	91%	38.990	-	744,000
	6AV		-	-	88%	-	34-1/8	648,000
	8AV		-	-	88%	-	34-1/8	872,000
EPW-6/8V Vipac Powder	6BV	43	0.5605-0.5620	-	86.33%	39.000	34-1/4	757,000
	6CV		0.5605-0.5620	-	86.90%	39.039	34-3/16	750,000
	8BV		0.5600-0.5610	-	87.39%	39.040	34-1/8	888,000
	8CV		0.5610-0.5620	-	88.86%	39.031	34-1/8	1,000,000
EPW-10/12V Vipac Powder	10AV	44	0.5620-0.5625	-	84.67%	39.017	34-1/4	1,210,000
	10BV		0.5610-0.5625	-	84.67%	39.010	34-1/4	1,107,000
	12AV		0.5600-0.5610	-	85.06%	38.970	29-1/2	1,482,000
	12BV		0.5615-0.5625	-	83.63%	38.943	29-1/2	1,351,000
EPW-12V Vipac Powder	12CV	47-52	0.5610-0.5625	-	83.83%	39.015	29-7/8	1,222,000
	12DV		0.5655-0.5665	-	85.00%	38.995	29-1/2	1,357,000
	12GV		0.5655-0.5660	-	83.00%	39.008	29-7/8	1,123,000
	12FV		0.5640-0.5650	-	84.97%	39.021	29-1/2	1,260,000
EX-12A Vipac Powder Large Cored Pellets (Liner)	12GV	54-58	0.5660-0.5680	-	-	39.027	-	1,070,000
	12FV		0.5640-0.5670	-	-	39.050	-	1,030,000
	12FC		-	-	-	-	-	1,360,000
	12KCF		-	-	-	-	-	1,170,000

*There is approximately 10 percent variation in the heat flux values reported for the fuel rods from EPW-6/8 and EPW-6/8A in the various program reports. These variations arise from differences between physics and gamma scan indications of the power split among the rods and changes in the PWL axial peaking factors based on measurements performed midway through the program.



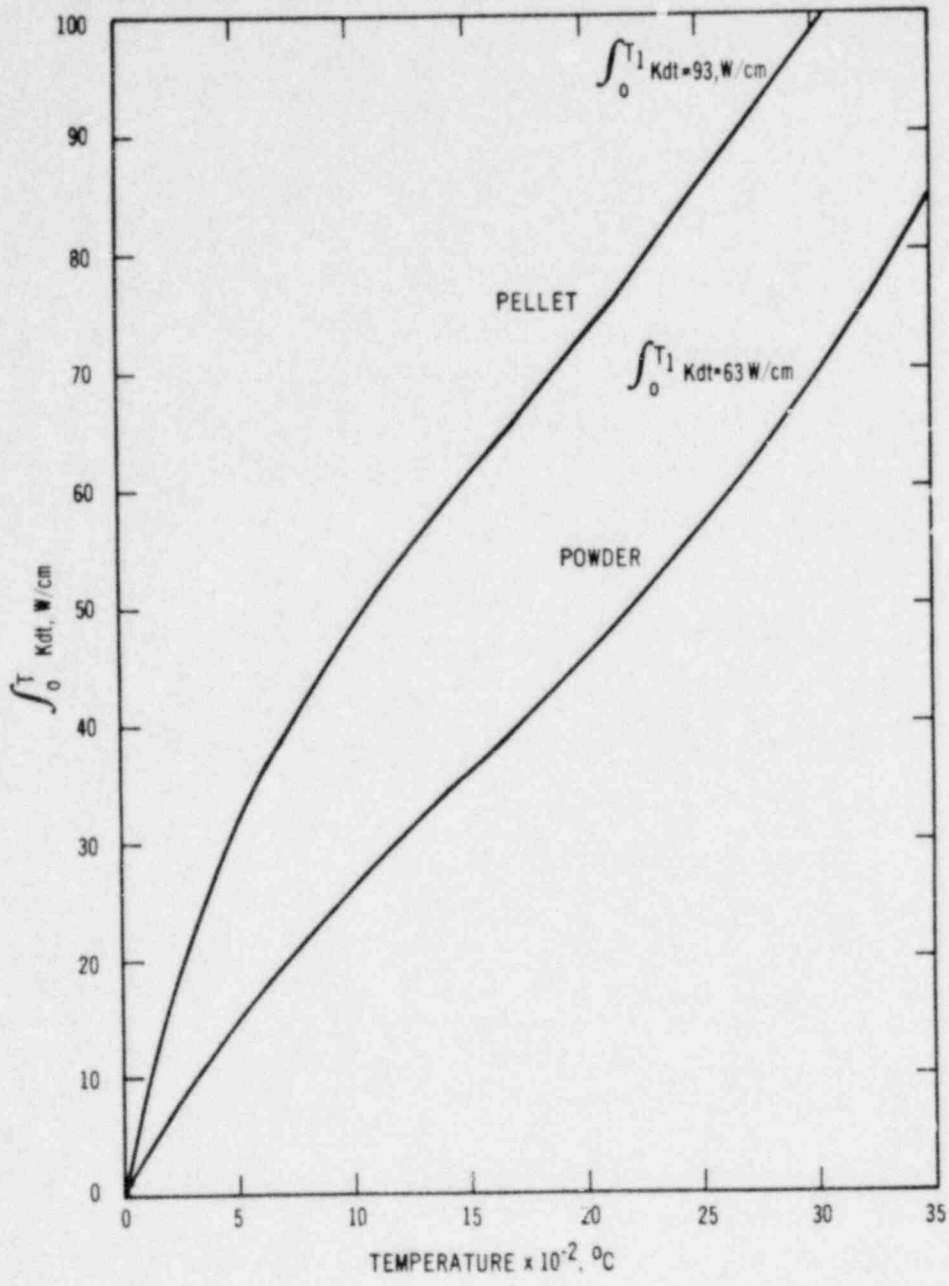


FIGURE 1. $\int K dt$ VERSUS TEMPERATURE

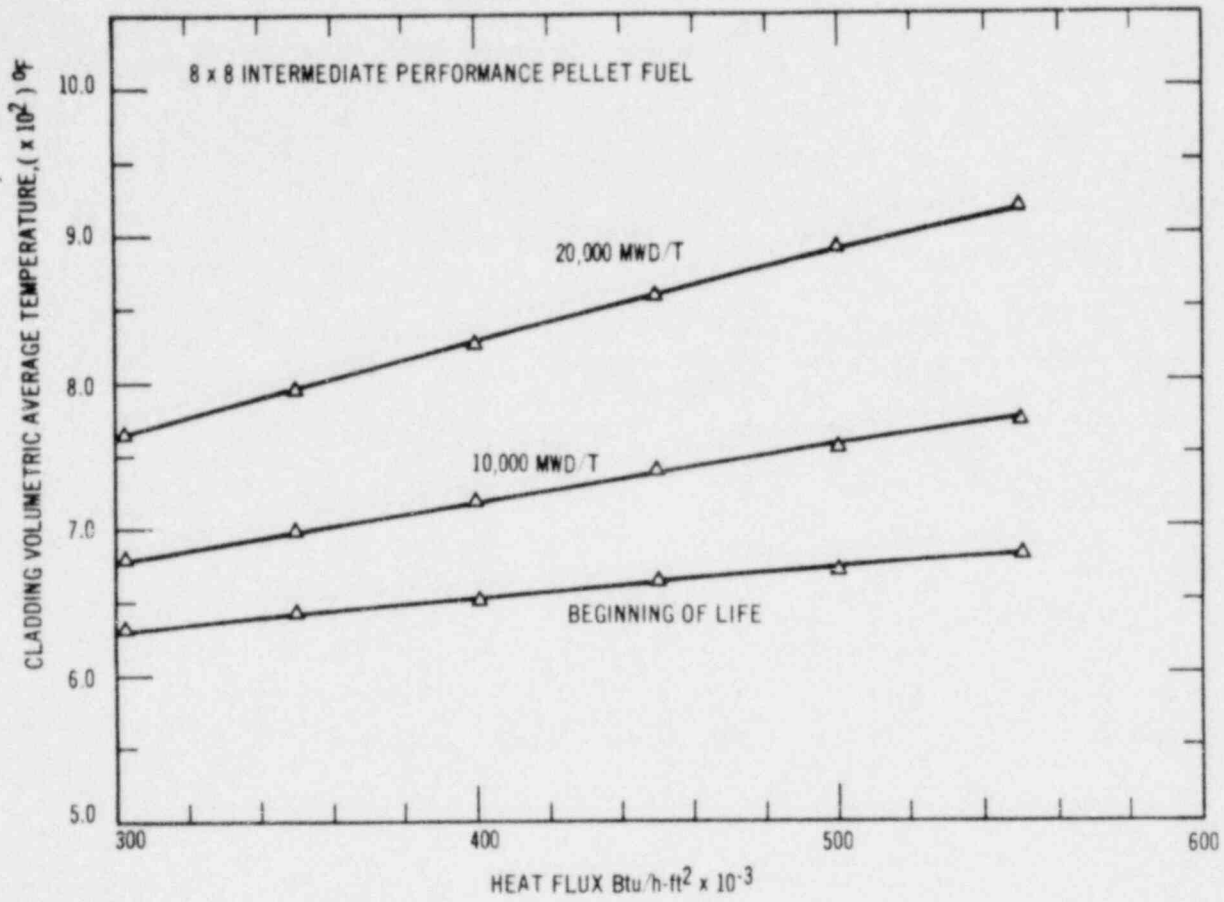


FIGURE 2. CLADDING VOLUMETRIC AVERAGE TEMPERATURE VERSUS HEAT FLUX

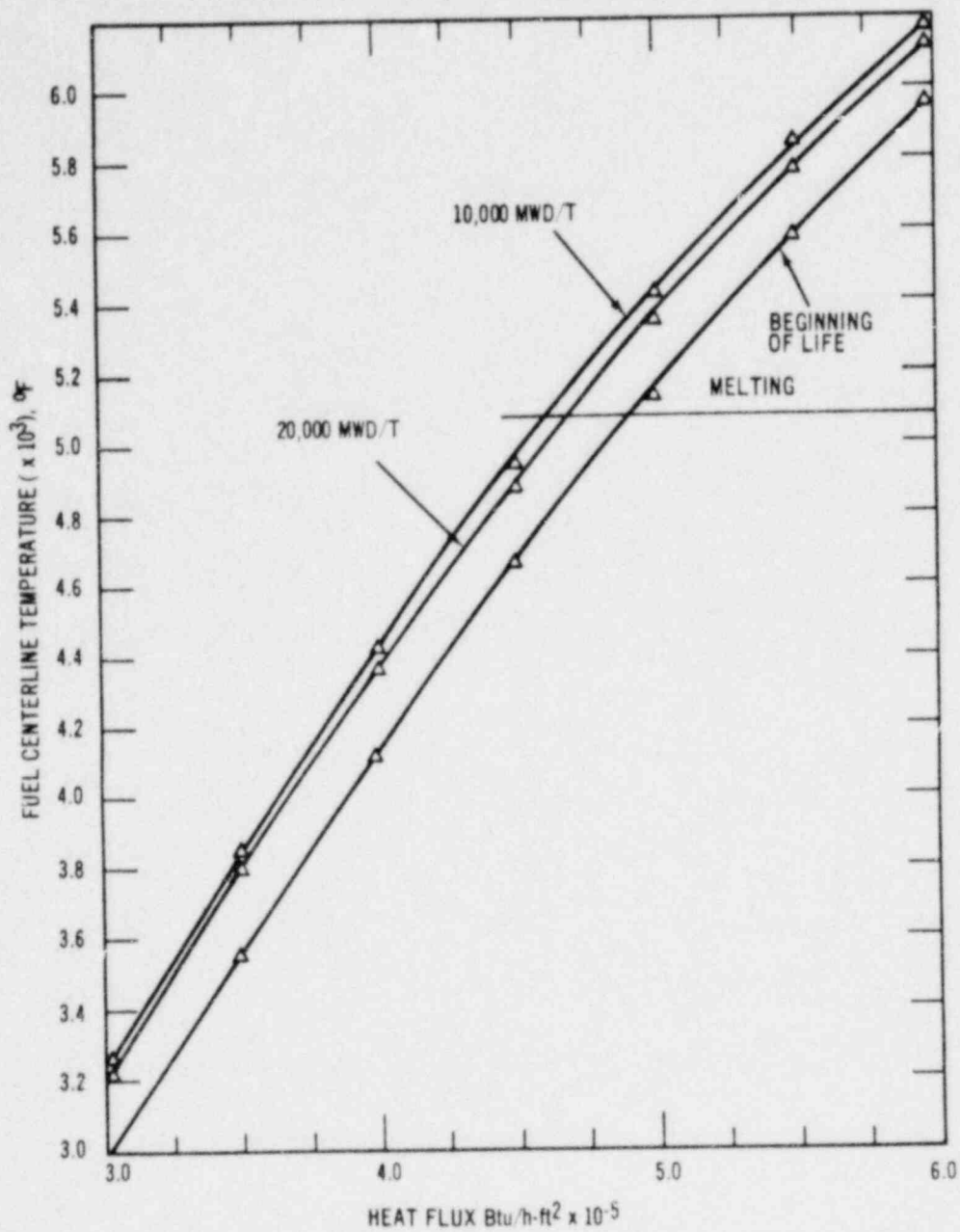


FIGURE 3. FUEL CENTERLINE TEMPERATURE VERSUS HEAT - FLUX, INTERMEDIATE PERFORMANCE PELLET FUEL

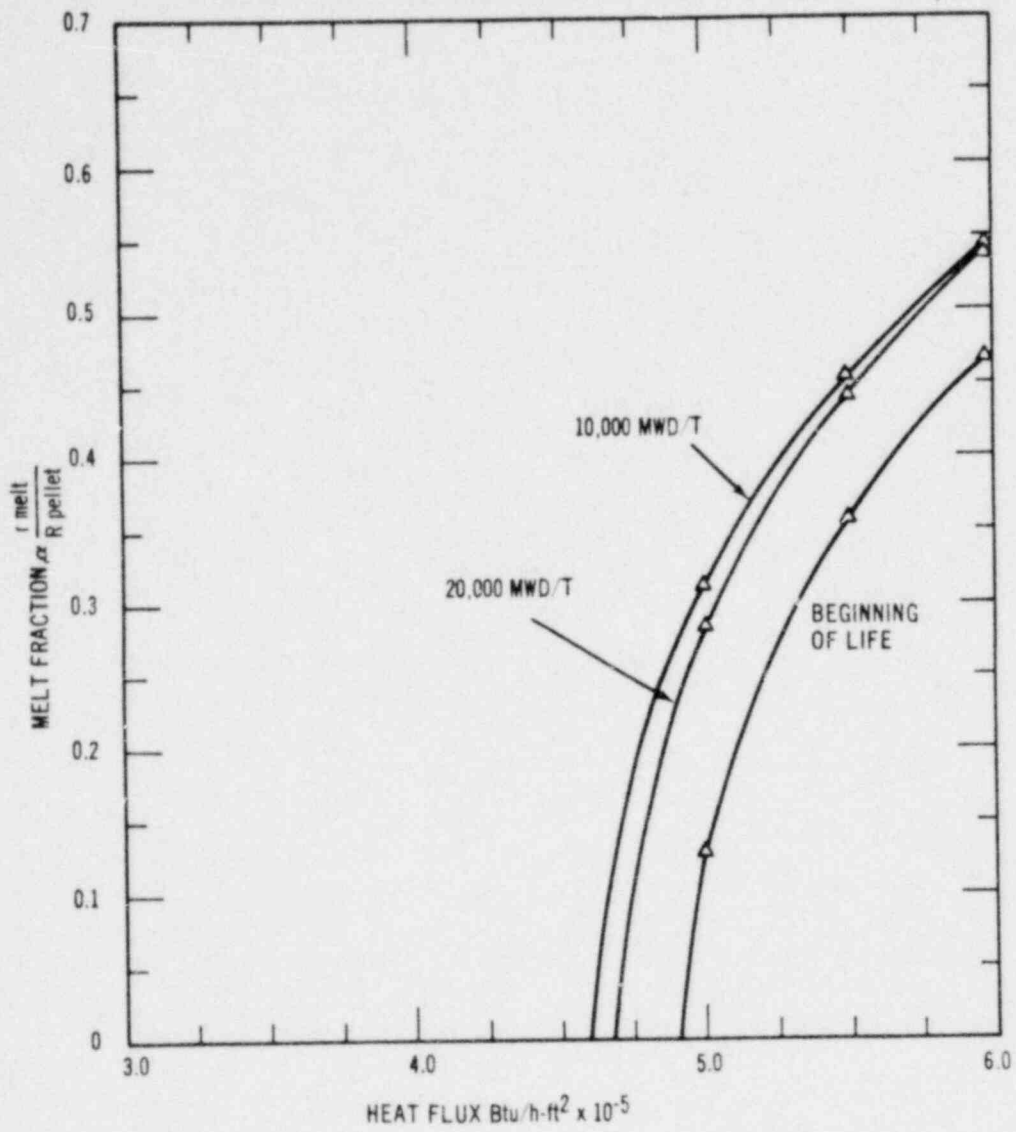


FIGURE 4. MELT FRACTION VERSUS HEAT FLUX - INTERMEDIATE PERFORMANCE PELLETT FUEL

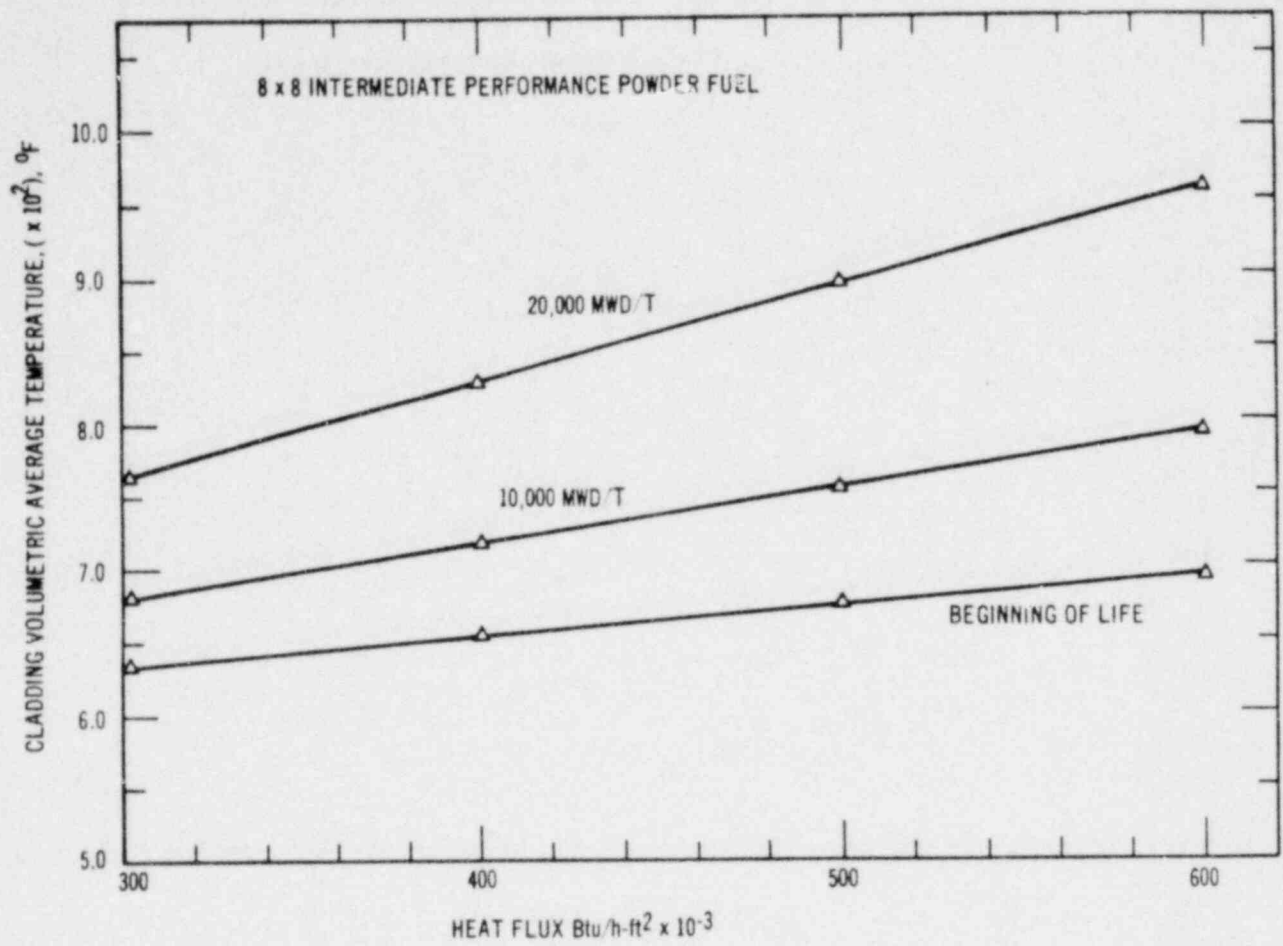


FIGURE 5. CLADDING VOLUMETRIC AVERAGE TEMPERATURE VERSUS HEAT FLUX

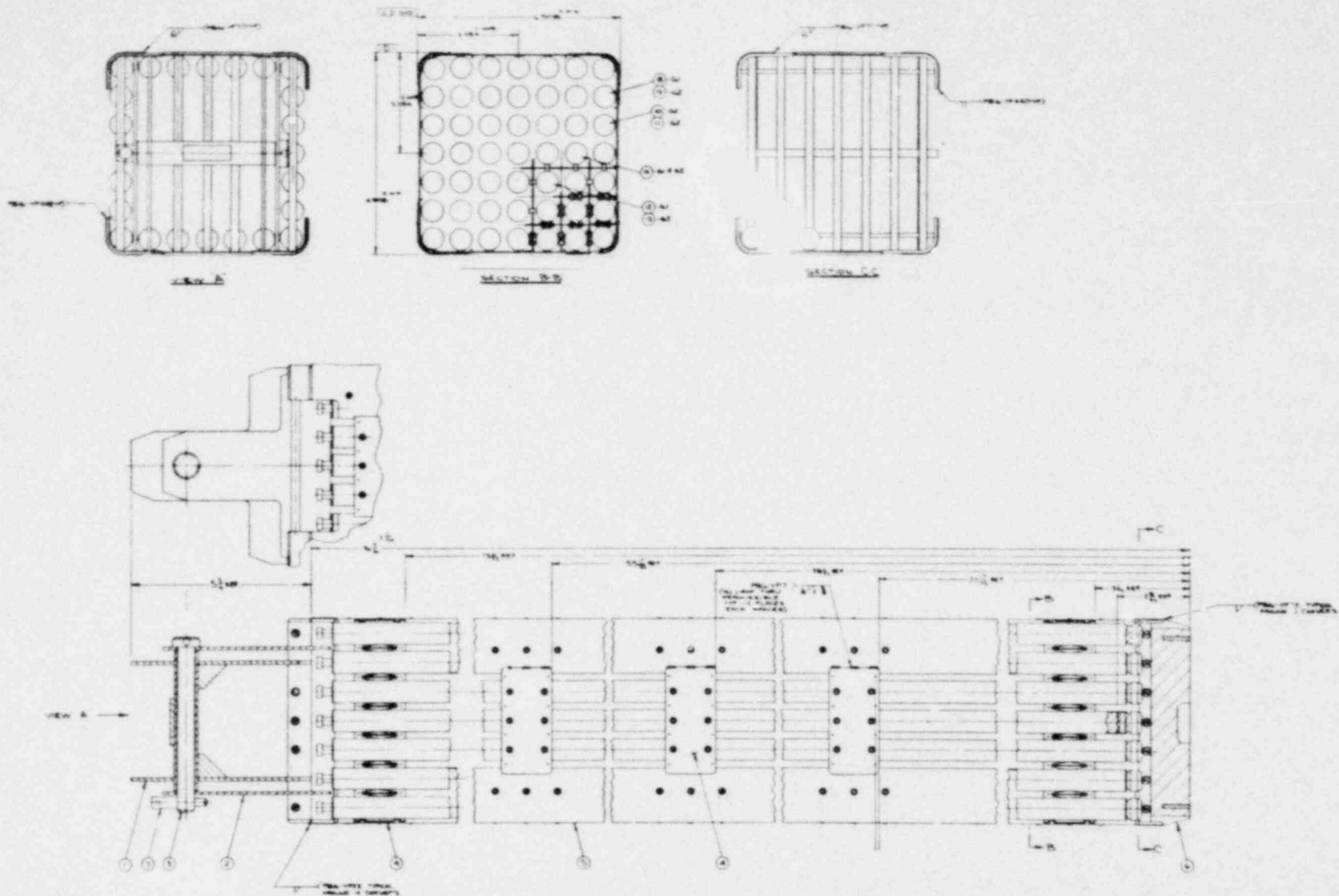
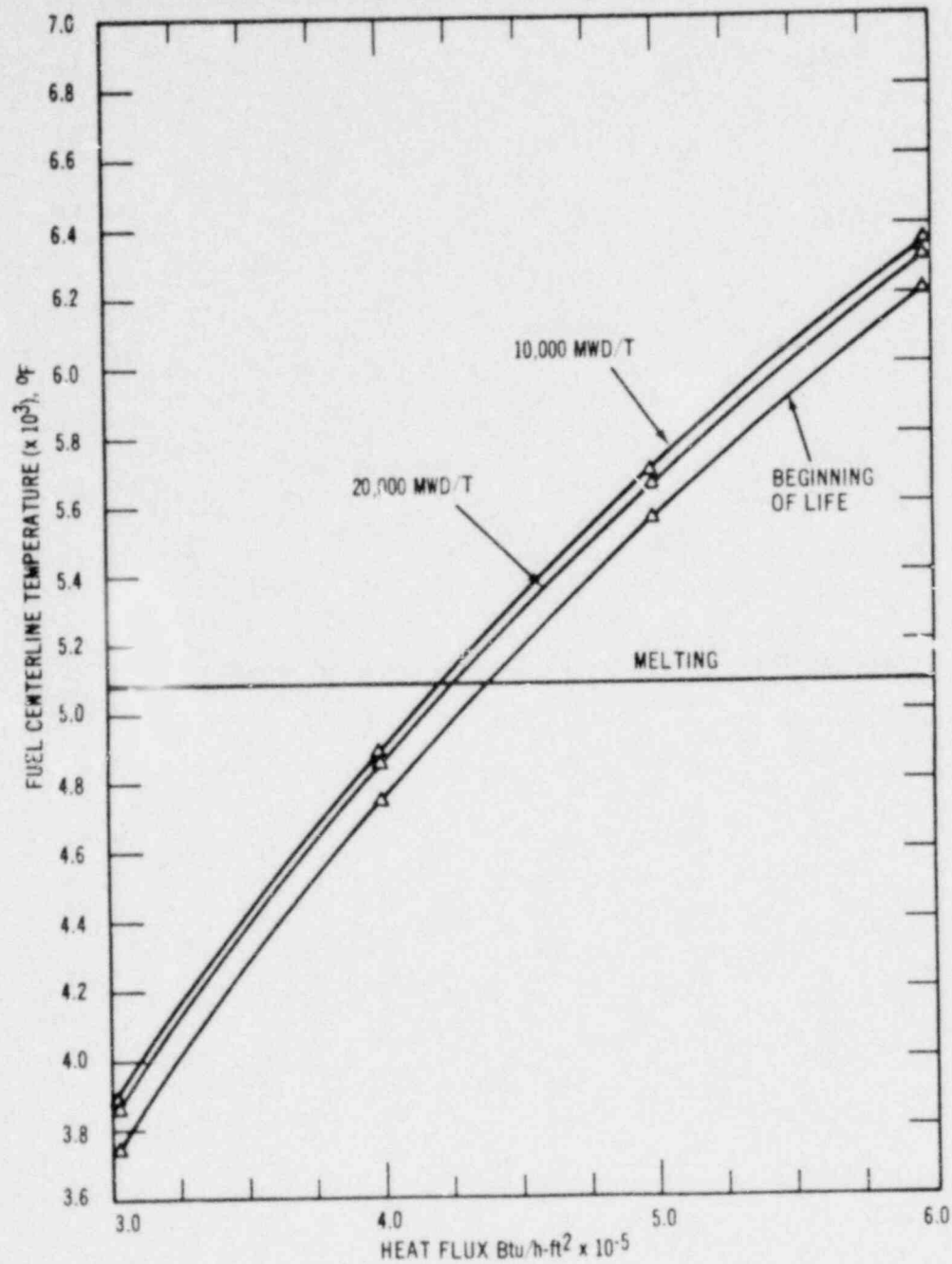


FIGURE 5-6. DRAWING OF 7 x 7 FUEL LATTICE CENTERMELT BUNDLE



• FIGURE 6. FUEL CENTERLINE TEMPERATURE VERSUS HEAT FLUX - INTERMEDIATE PERFORMANCE POWDER FUEL

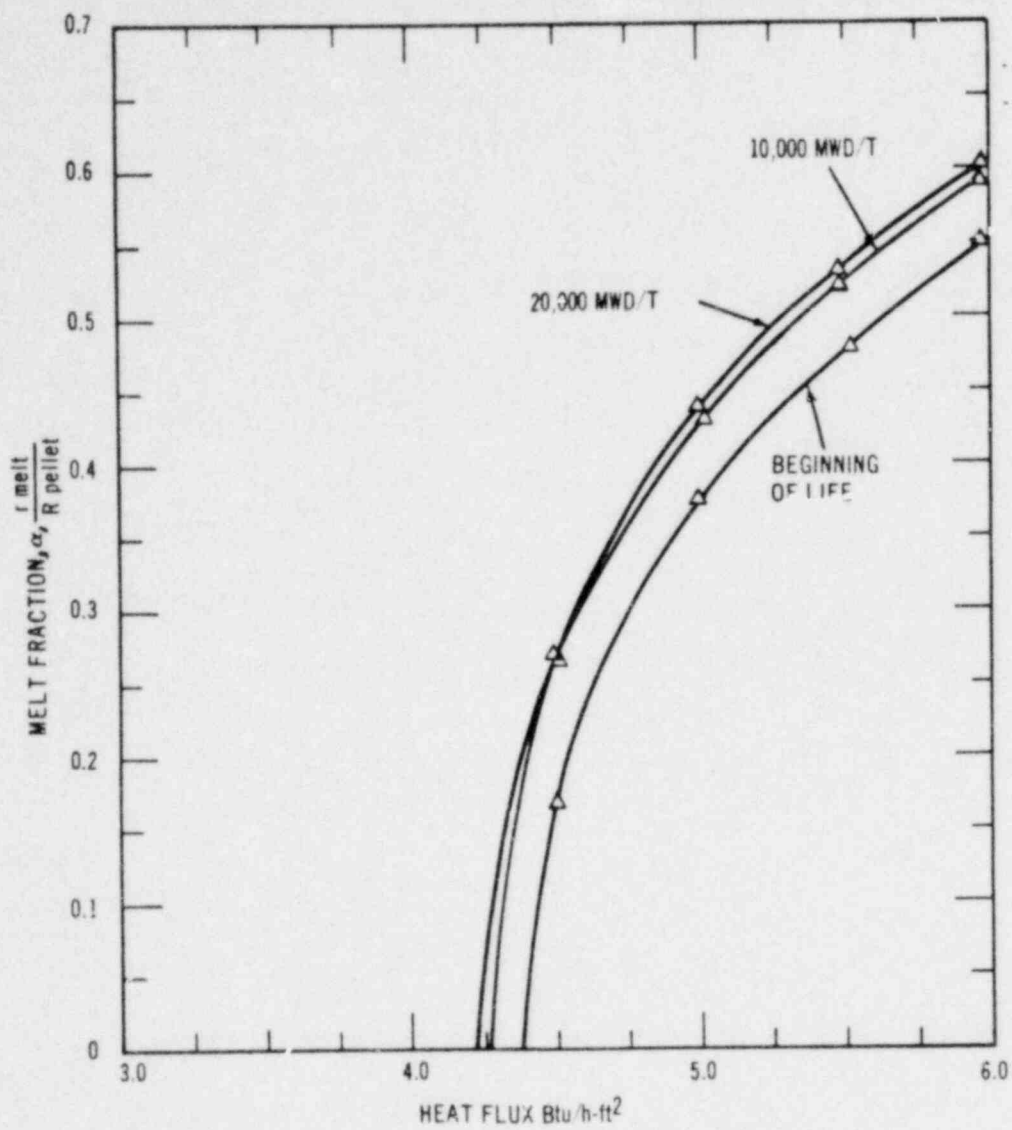


FIGURE 7. UO₂ MELT FRACTION VERSUS HEAT FLUX - INTERMEDIATE PERFORMANCE FUEL - POWDER

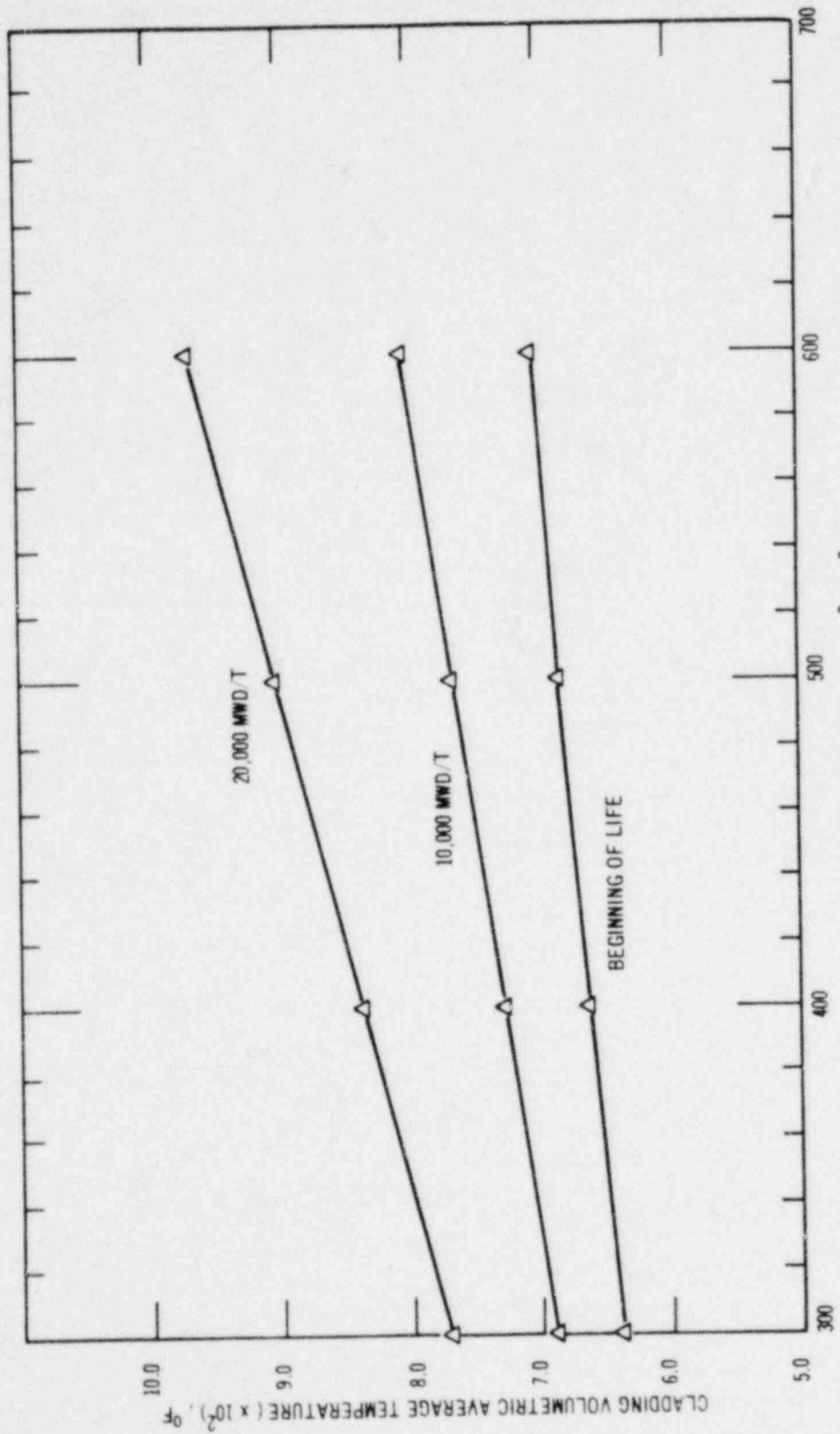


FIGURE 8. CLADDING VOLUMETRIC AVERAGE TEMPERATURE VERSUS HEAT FLUX
7 x 7 ADVANCED PERFORMANCE POWDER FUEL

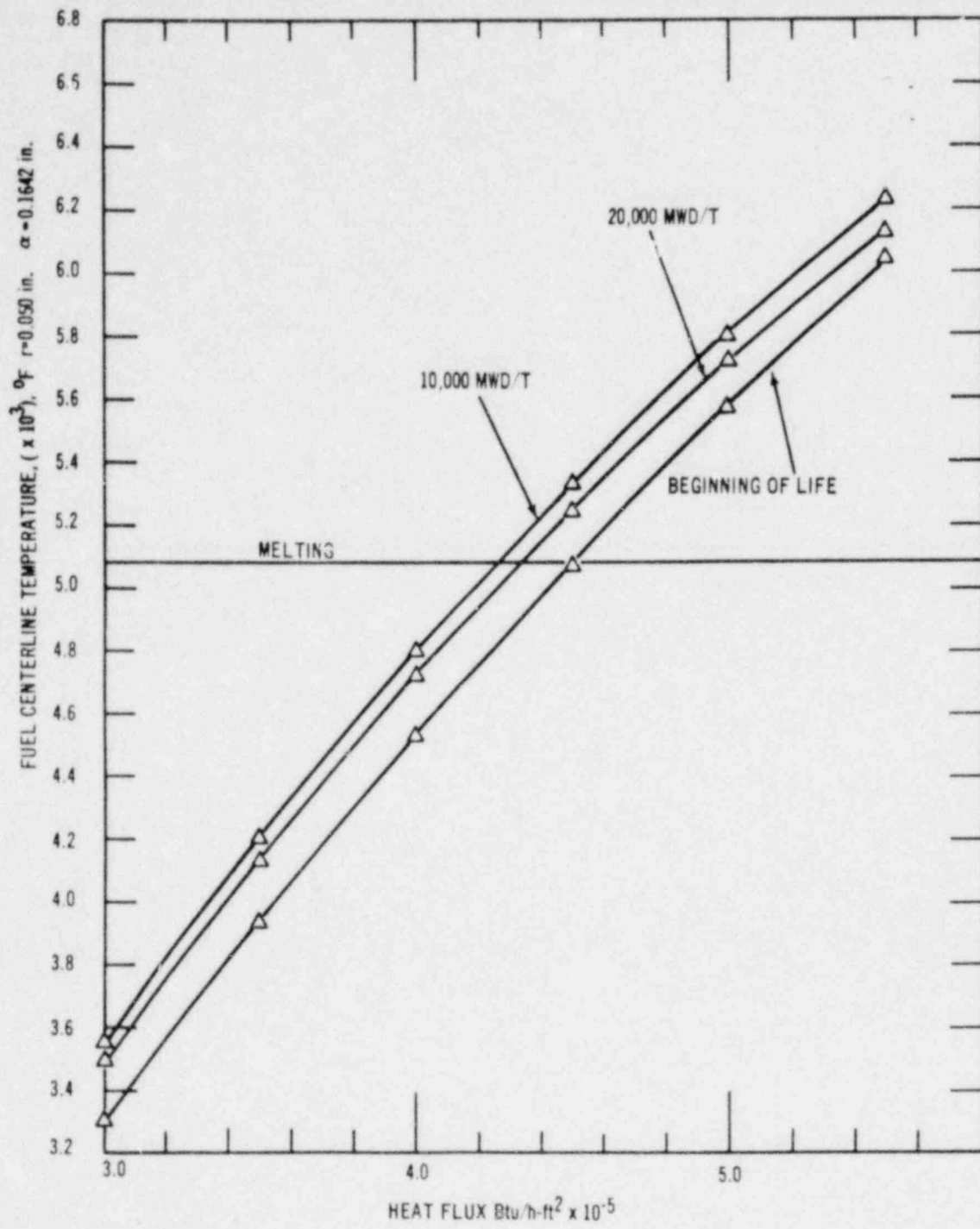


FIGURE 9. FUEL TEMPERATURE VERSUS Q/A_p HIGH PERFORMANCE PELLETT FUEL

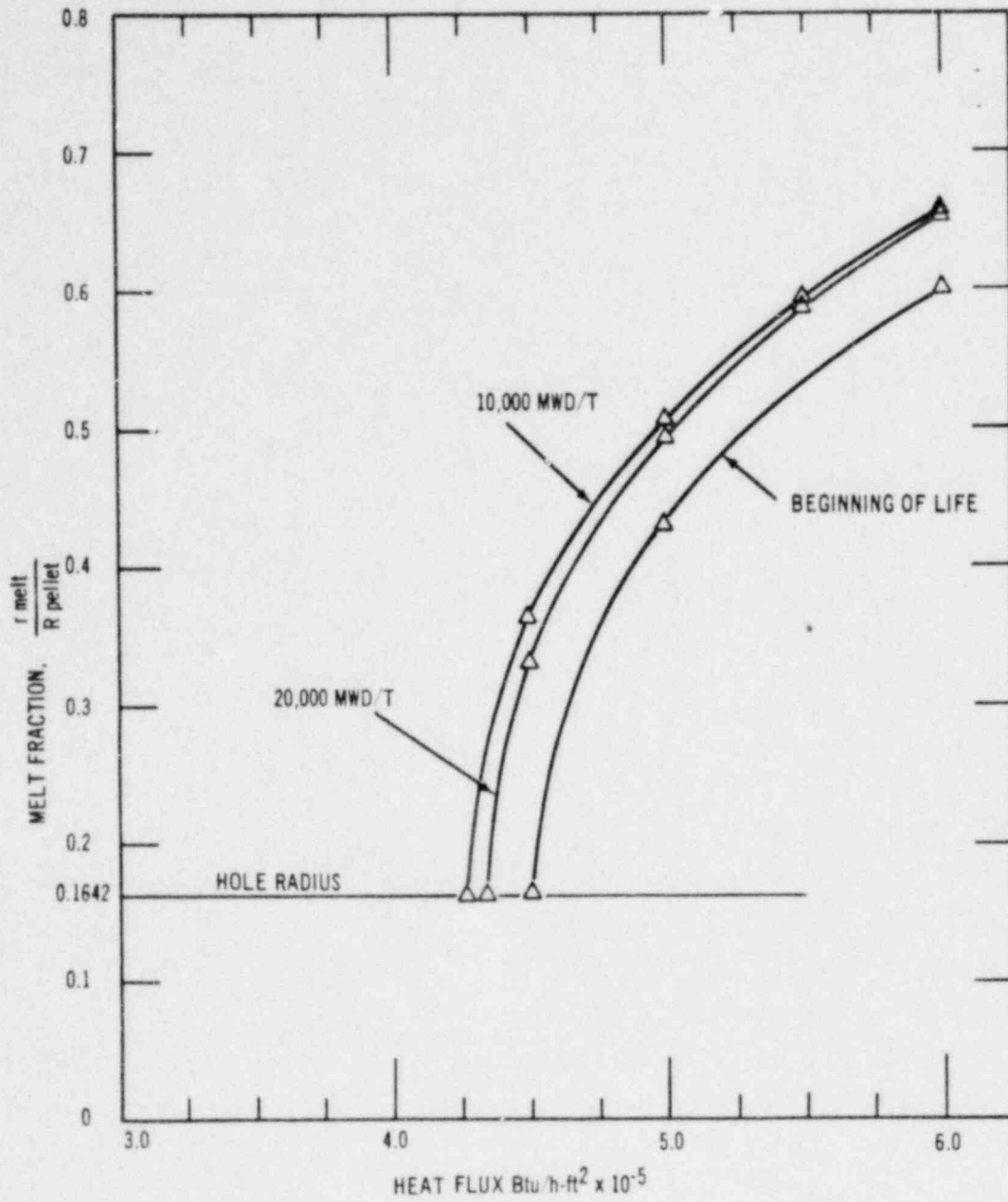


FIGURE 10. UO₂ MELT FRACTION VERSUS HEAT FLUX, HIGH PERFORMANCE PELLET FUEL, 0.100 in. CENTERLINE HOLE, $\alpha = 0.1642$

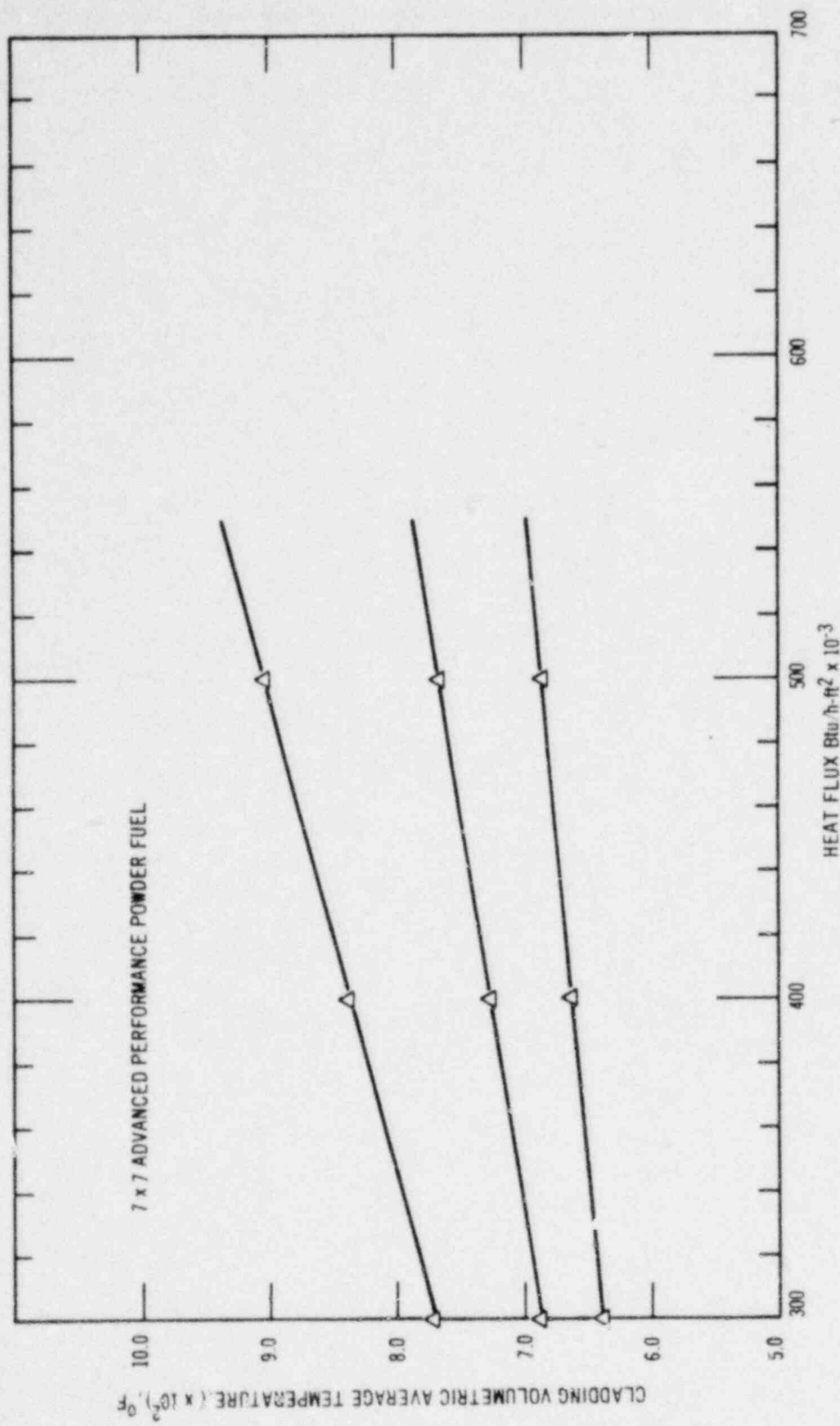


FIGURE 11. CLADDING VOLUMETRIC AVERAGE TEMPERATURE VERSUS HEAT FLUX

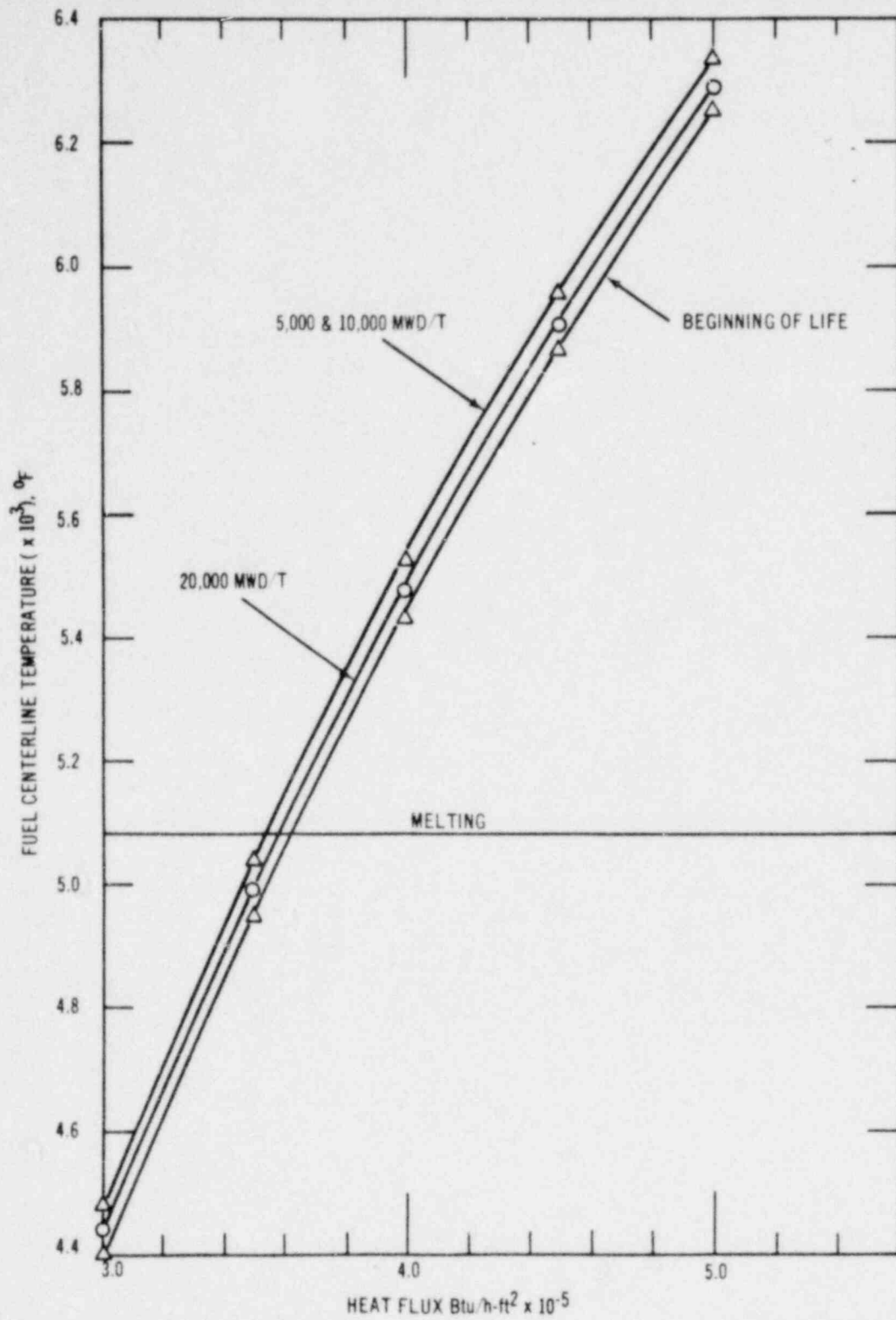


FIGURE 12. FUEL CENTERLINE VERSUS Q/A , HIGH PERFORMANCE POWDER FUEL

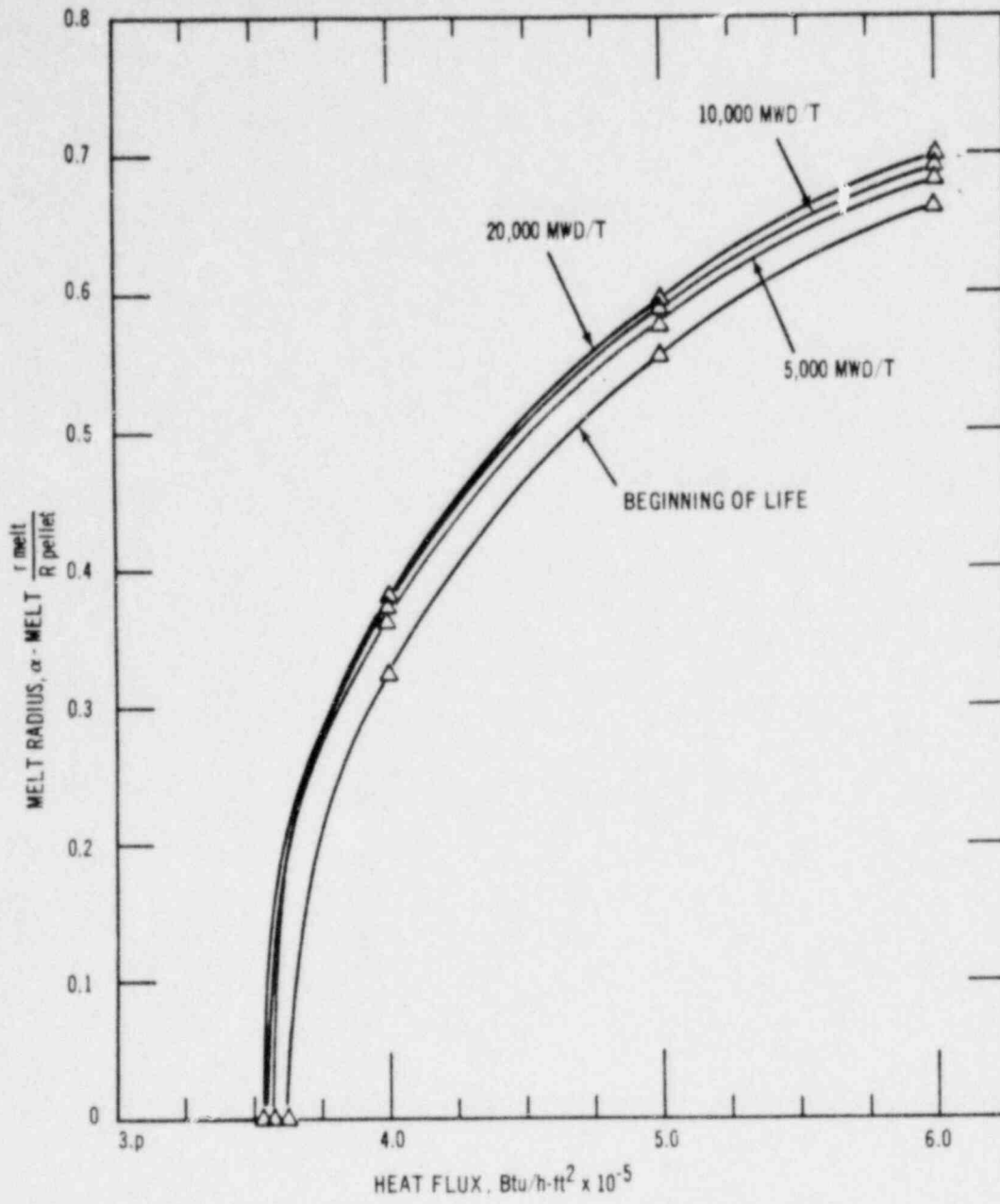


FIGURE 13. UO₂ MELT FRACTION VERSUS HEAT FLUX, HIGH PERFORMANCE POWDER FUEL

D 0.13	A 1.60	B 1.68	B 1.67	B 1.68	A 1.60	D 0.13
A 1.60	A 1.42	D 0.10	D 0.10	D 0.10	A 1.42	A 1.60
B 1.68	D 0.10	C 1.71	D 0.09	C 1.71	D 0.10	B 1.68
B 1.67	D 0.10	D 0.09	C 1.65	D 0.09	D 0.10	B 1.67
B 1.68	D 0.10	C 1.71	D 0.09	C 1.71	D 0.10	B 1.68
A 1.60	A 1.42	D 0.10	D 0.10	D 0.10	A 1.42	A 1.60
D 0.13	A 1.60	B 1.68	B 1.67	B 1.68	A 1.60	D 0.13

Type A U-235 Enrichment = 0.043
 Type B U-235 Enrichment = 0.050
 Type C U-235 Enrichment = 0.056
 Type D U-235 Enrichment = 0.0022 (Depleted)

Figure 14 - Individual Fuel Rod Relative Powers in the 7 x 7 Center-melt Bundle. Beginning of Life. Average Rod Power = 1.0

D 0.13	A 1.65	B 1.75	B 1.73	B 1.73	B 1.74	A 1.63	D 0.13
A 1.65	A 1.53	D 0.10	D 0.10	D 0.10	D 0.10	A 1.49	A 1.63
B 1.75	D 0.10	D 0.10	C 1.79	D 0.10	C 1.81	D 0.10	B 1.74
B 1.73	D 0.10	C 1.79	D 0.09	C 1.72	D 0.10	D 0.10	B 1.73
B 1.73	D 0.10	D 0.10	C 1.72	D 0.09	C 1.79	D 0.10	B 1.73
B 1.74	D 0.10	C 1.81	D 0.10	C 1.79	D 0.10	D 0.10	B 1.75
A 1.63	A 1.49	D 0.10	D 0.10	D 0.10	D 0.10	A 1.53	A 1.65
D 0.13	A 1.63	B 1.74	B 1.73	B 1.73	B 1.75	A 1.65	D 0.13

Type A U-235 Enrichment = 0.043
 Type B U-235 Enrichment = 0.050
 Type C U-235 Enrichment = 0.056
 Type D U-235 Enrichment = 0.0022 (Depleted)

Figure 15 - Individual Fuel Rod Relative Powers in the 8 x 8 Center-melt Bundle. Beginning of Life. Average Rod Power = 1.0

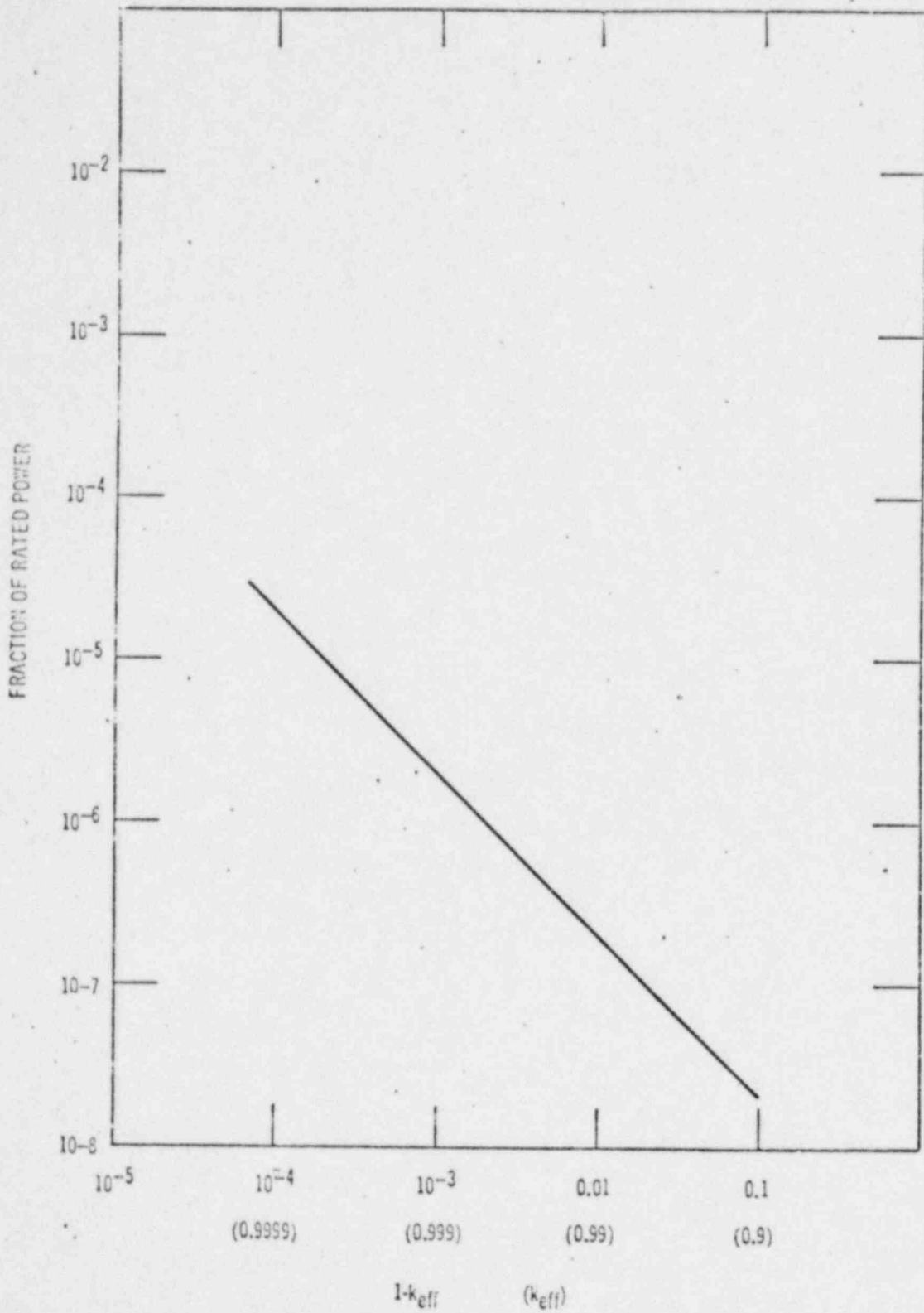


FIGURE 16. BRP SOURCE AND MULTIPLICATION

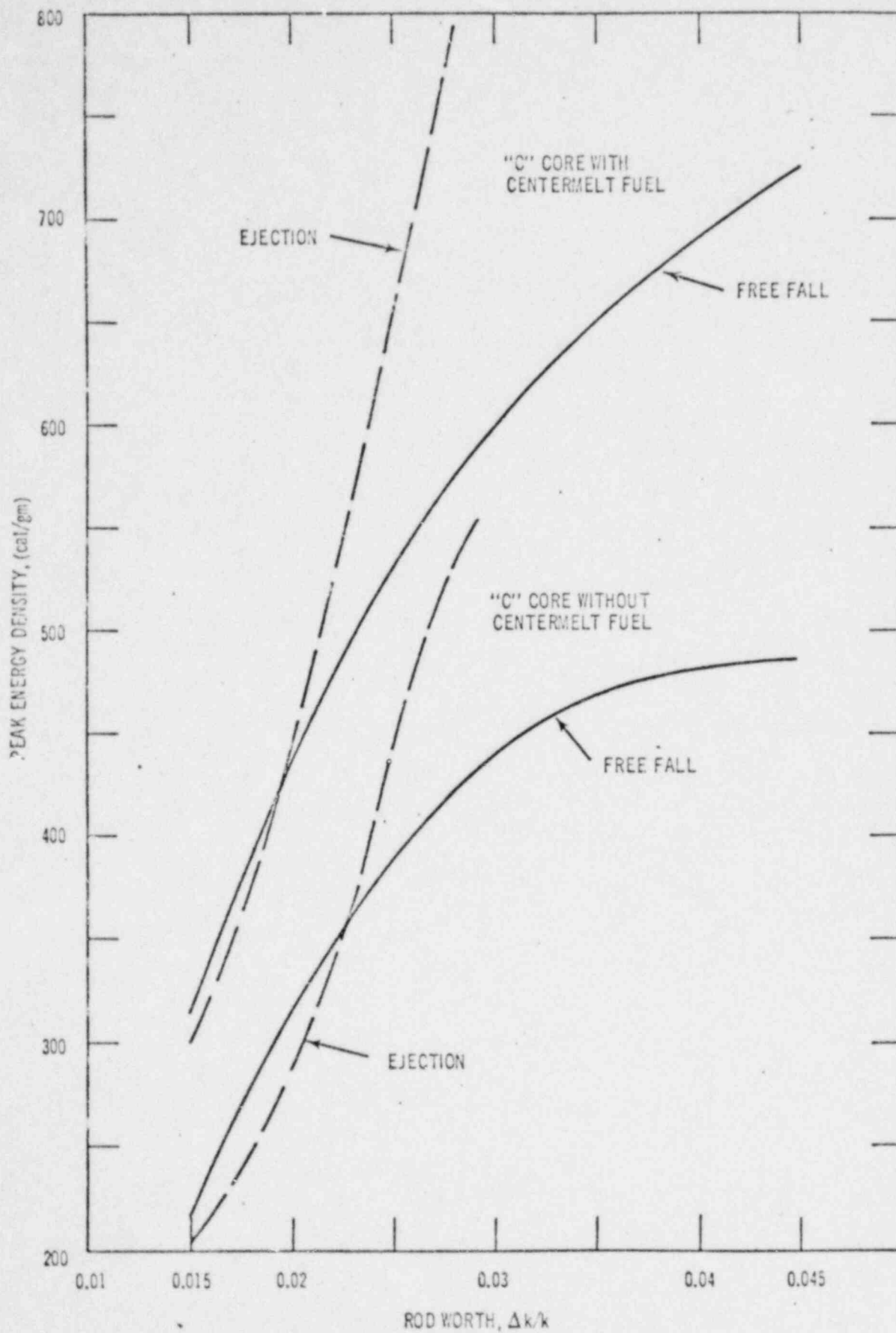
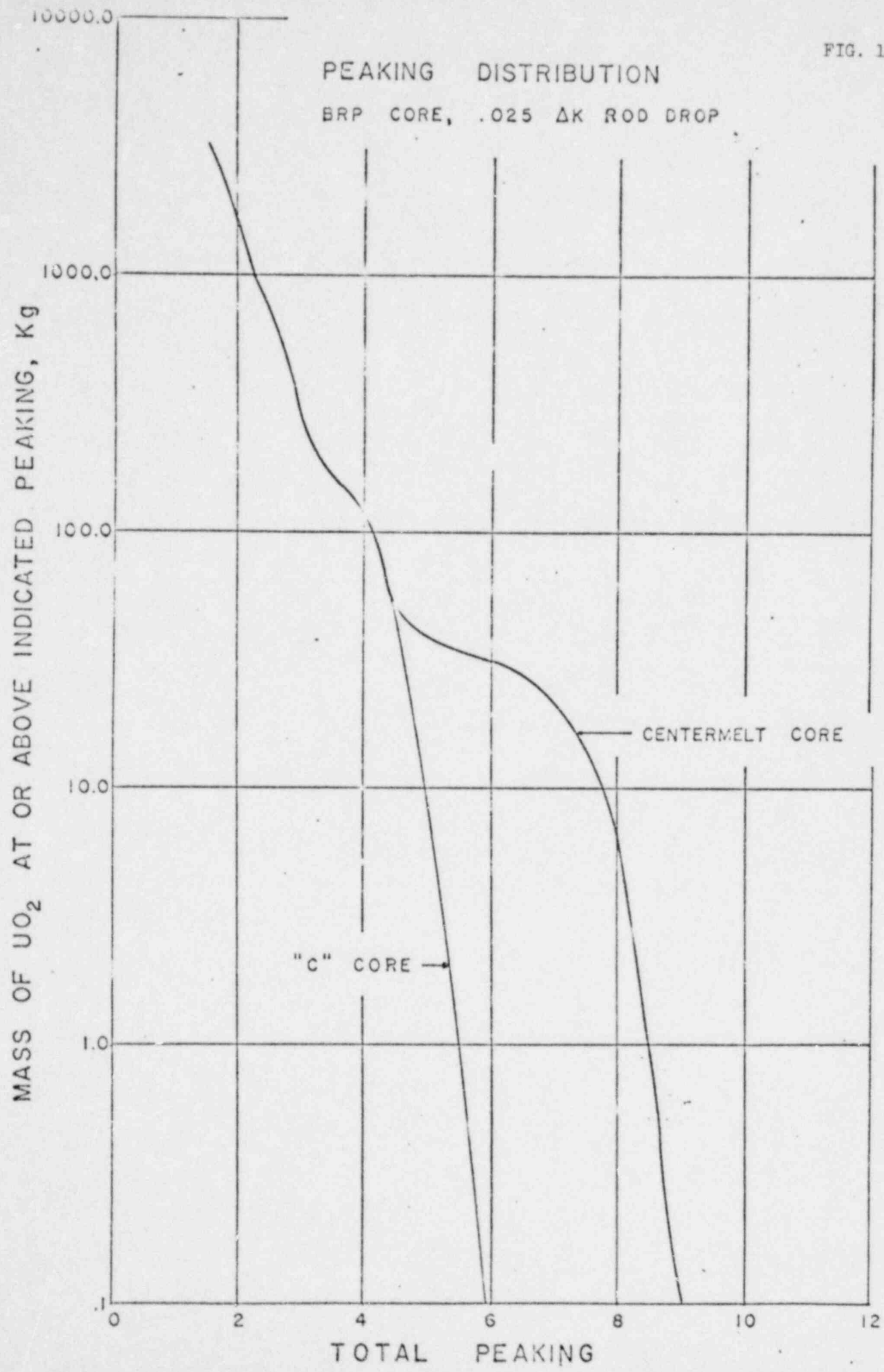


FIGURE 17. PEAK ENERGY IN ROD DROP AND EJECTION ACCIDENTS

FIG. 18

PEAKING DISTRIBUTION

BRP CORE, .025 ΔK ROD DROP



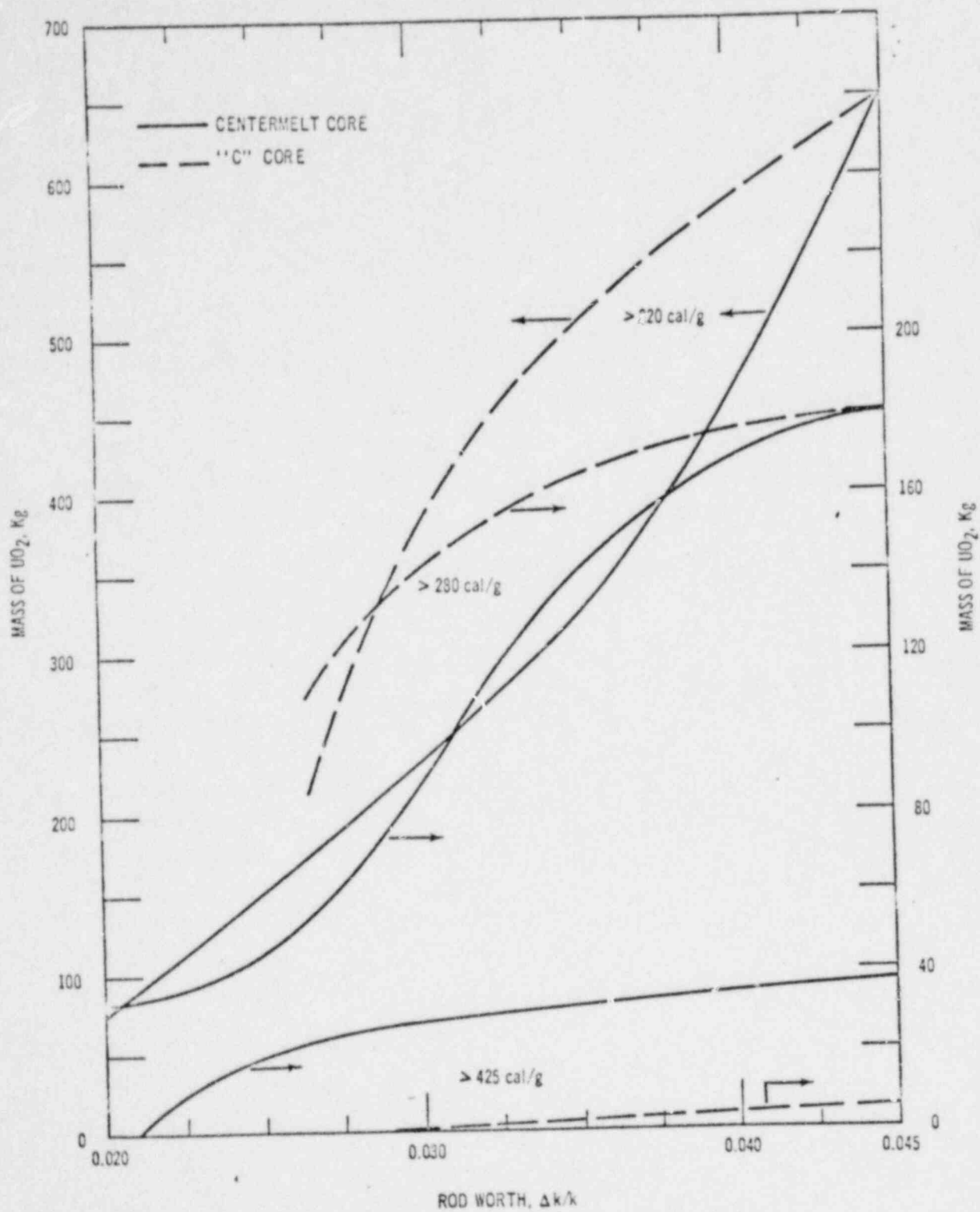


FIGURE 19. ROD DROP FINAL ENERGY DISTRIBUTION

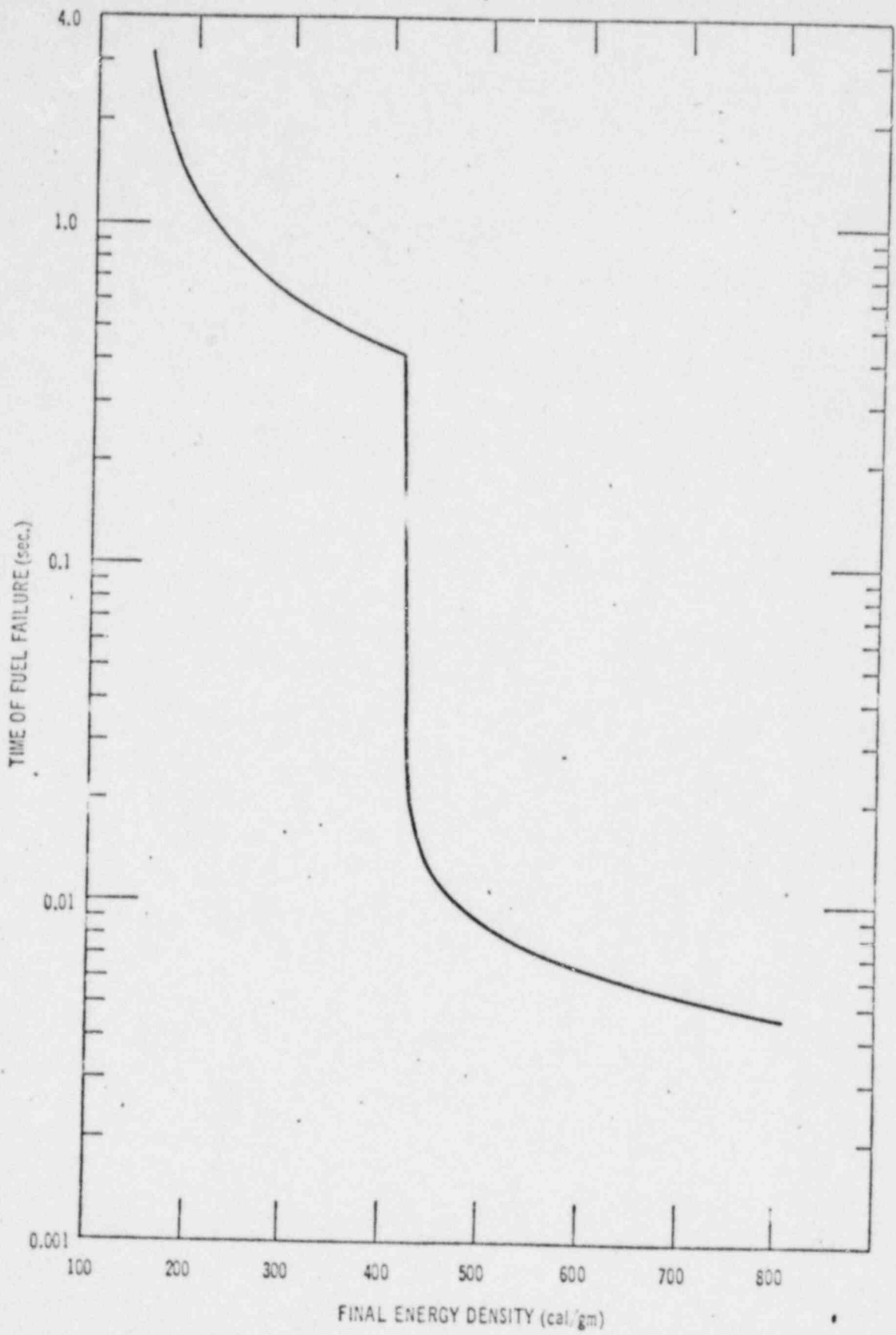


FIGURE 20. FUEL FAILURE SEQUENCE

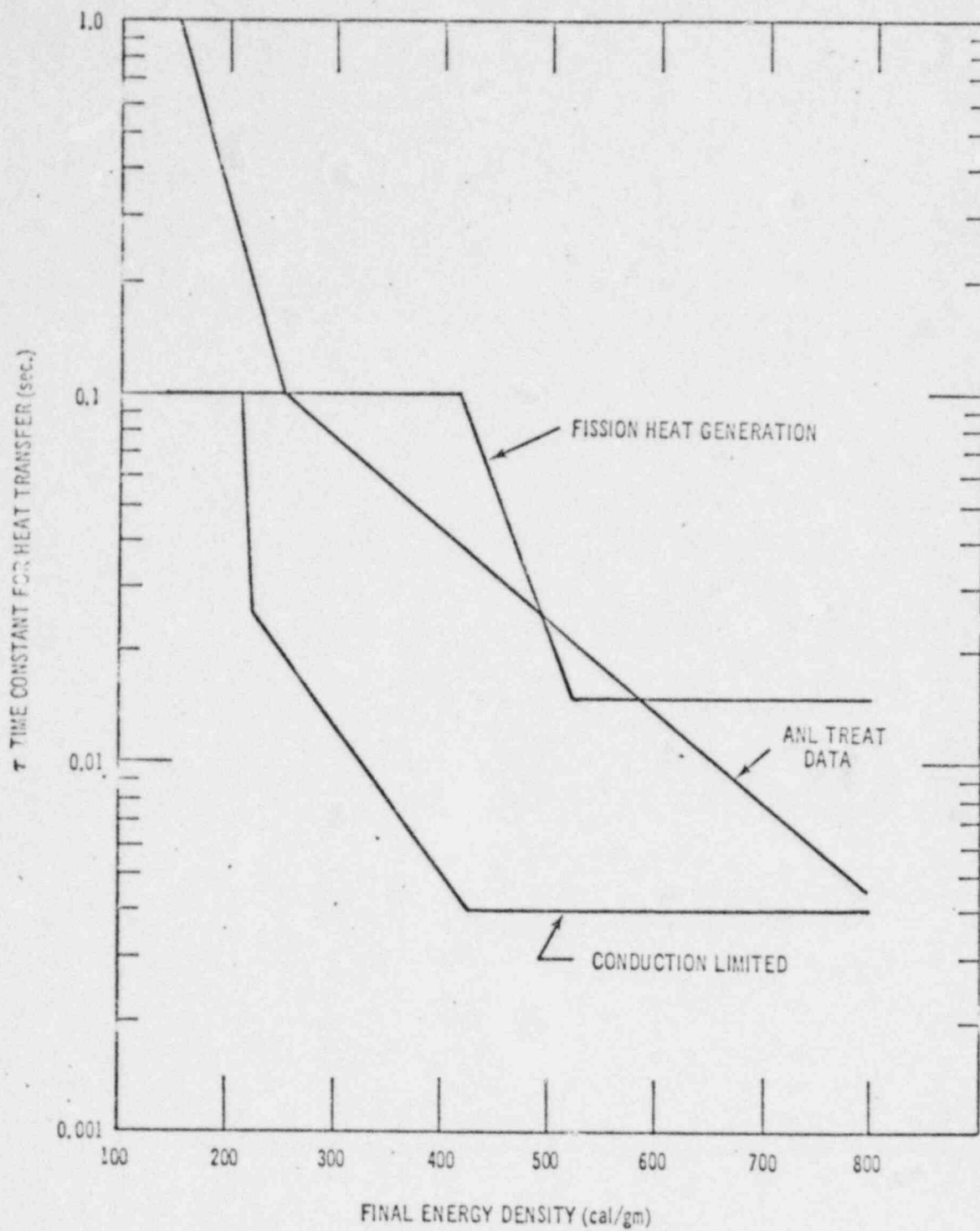


FIGURE 21. HEAT TRANSFER TIME CONSTANT

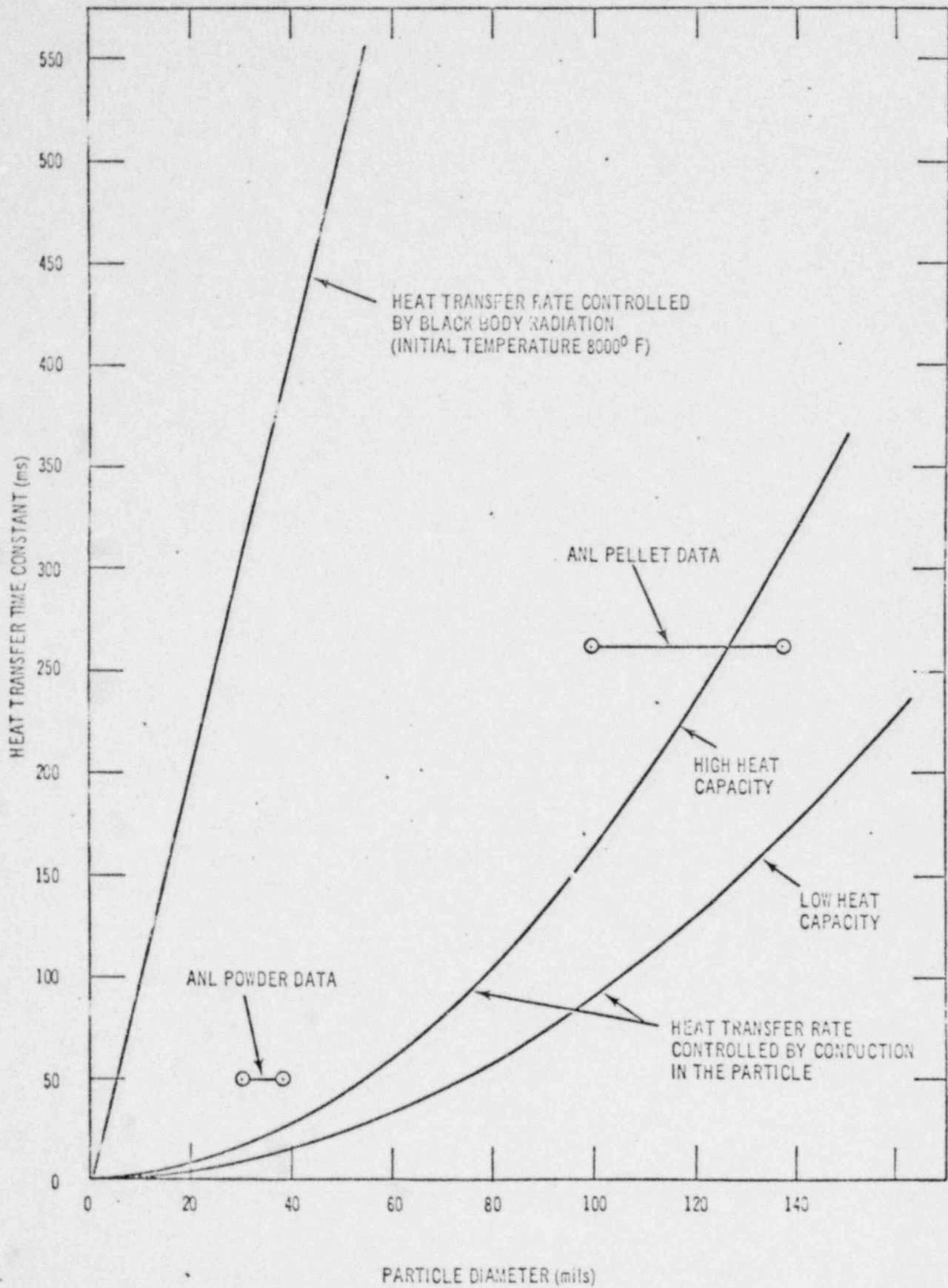


FIGURE 22. SPHERICAL PARTICLE HEAT TRANSFER

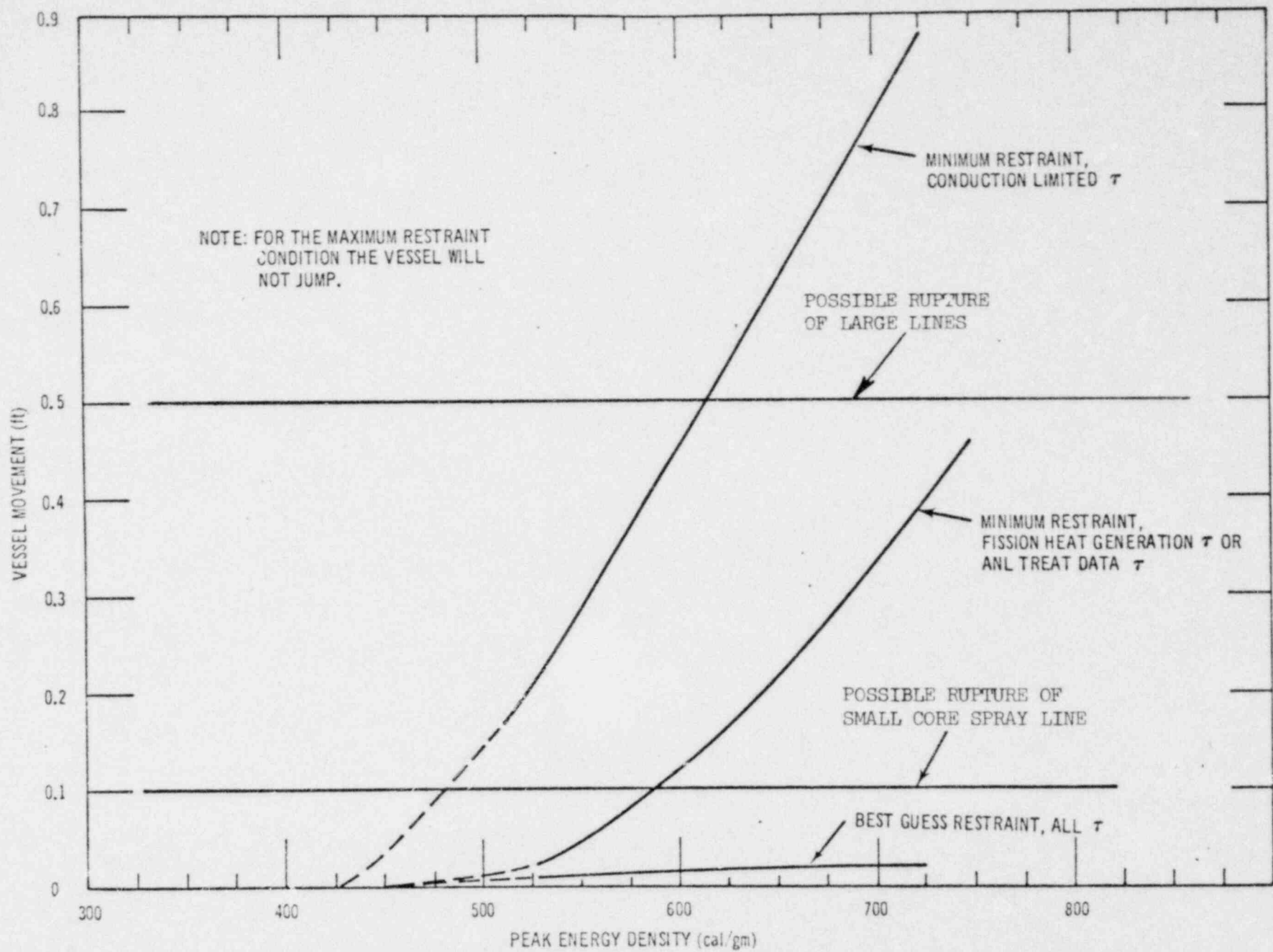


FIGURE 23. BRP VESSEL JUMP

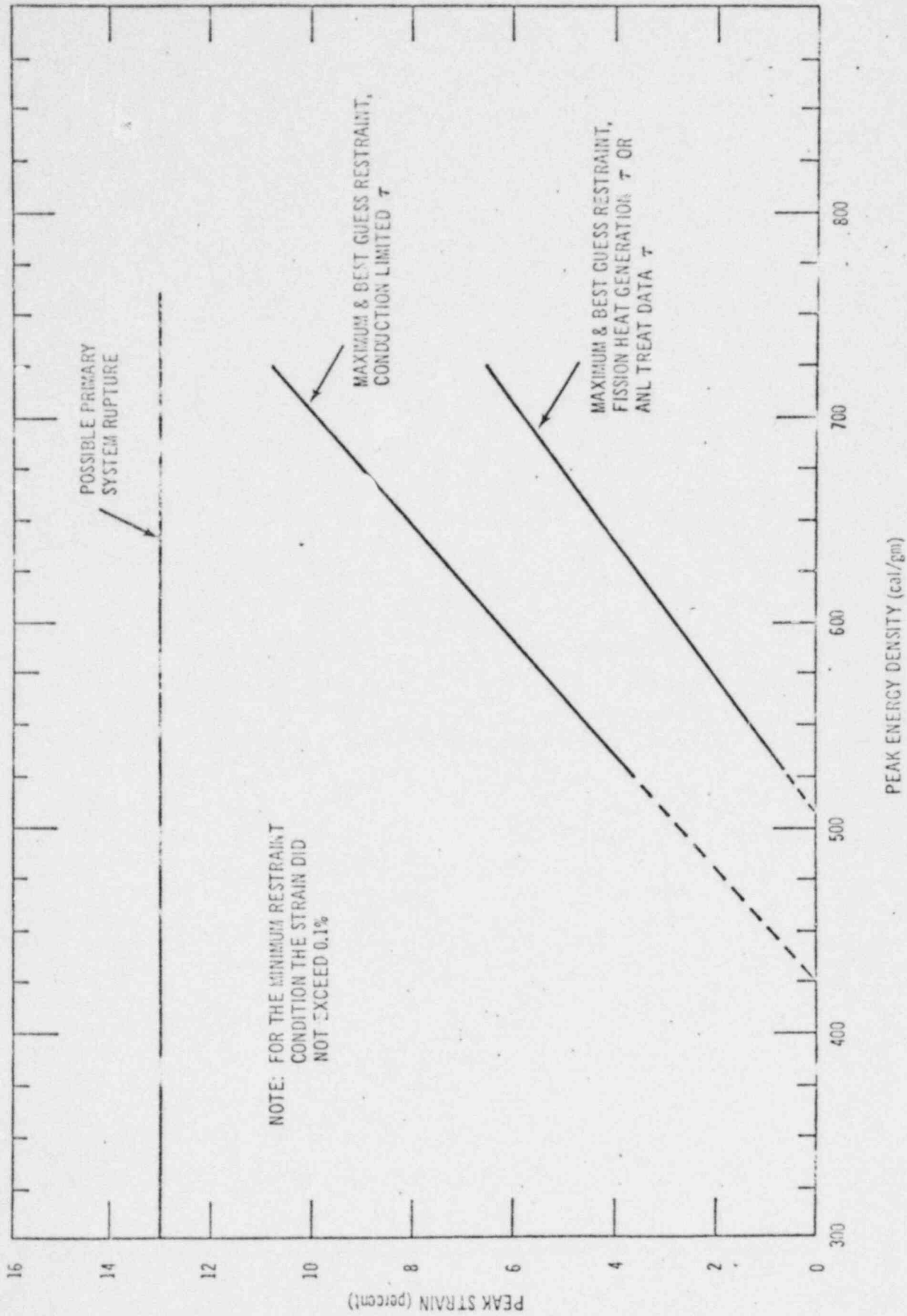


FIGURE 24. BRP VESSEL STRAIN

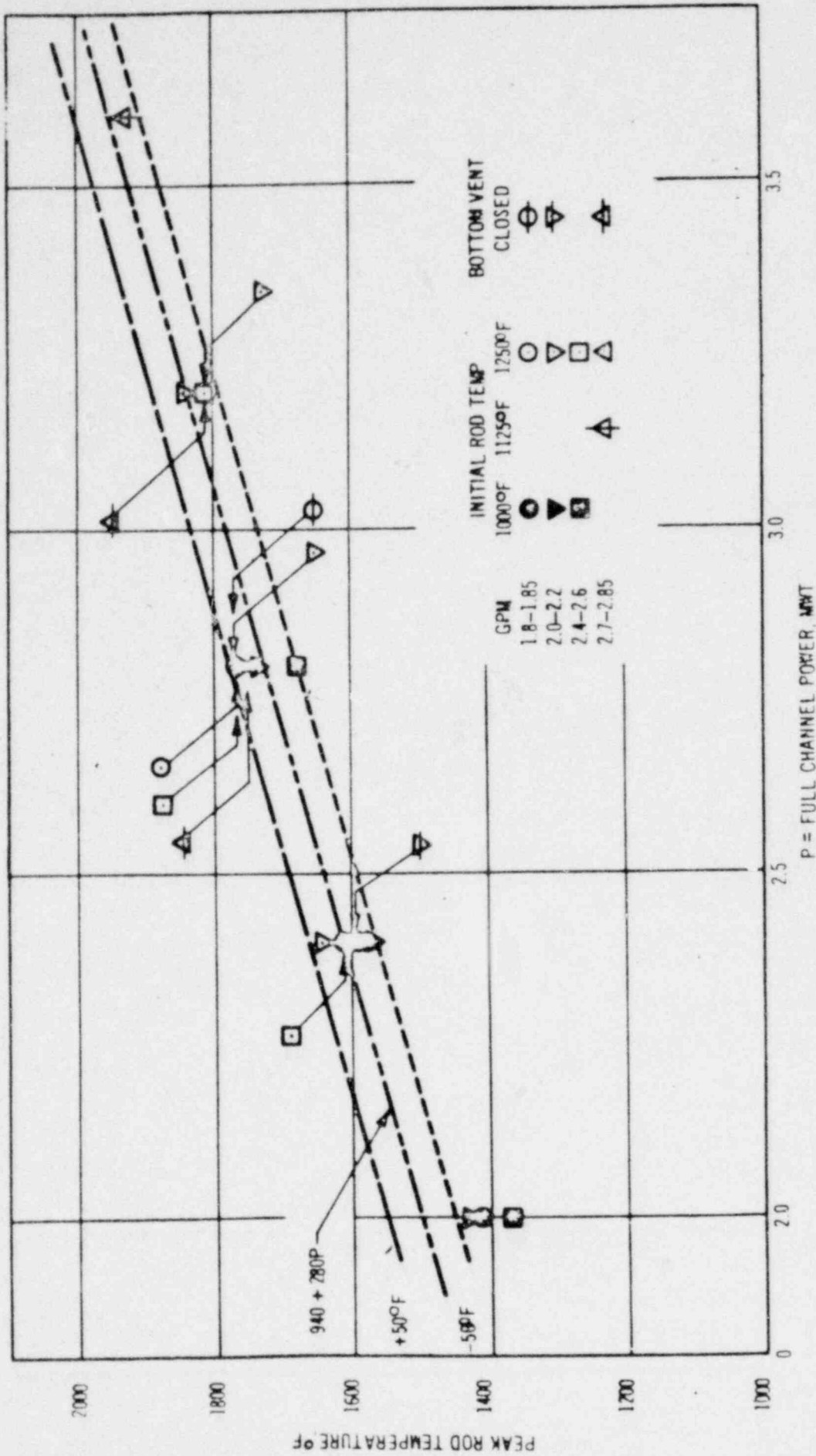


FIGURE 25. Highest Rod Peak Temperatures During Emergency Spray Cooling Transient

REFERENCES

1. BAW-1244, "Resonance Absorption in U-238 Metal and Oxide Rods," W. G. Pettus (1962).
2. NS&E 8, 497 (1960) E. Hellstrand, et al, "The Temperature Coefficient of the Resonance Integral for Uranium Metal and Oxide."
3. NS&E 11, 39 (1961) L. Dresner, "Some Remarks on the Effect of a Non-Uniform Temperature Distribution on the Temperature Dependence of Resonance Absorption."
4. WCAP-1434, "Multi-Region Reactor Lattice Studies Microscopic Lattice Parameters in Single and Multi-Region Cores," June 1961.
5. NS&E 19, 172 (1964) A. H. Spano, "Analysis of Doppler-Limited Excursions in a Water-Moderated Oxide Core."
6. L. Baker, Jr., R. O. Ivins, A. D. Tevebaugh, Chemical Engineering Division Summary Reports:
 - ANL 7325 - July-December 1966
 - 7225 - January-June 1966
 - 7125 - July-December 1965
 - 7055 - January-June 1965
7. Conway, Fincel, Hein, Trans. Amer. Nuclear Society, 6, No. 1 (1963) Page 153.

FROM: Consumers Paser Co. Jackson, Michigan Robert L. Hauster		DATE OF DOCUMENT: 5-26-67	DATE RECEIVED 5-31-67	NO: 1810
TO: Morris		LTR. X	MEMO:	REPORT:
CLASSIF.: V	POST OFFICE	ORIG. 3	CC: Orig & 19 conf'd cys	OTHER:
REG. NO.	FILE CODE: 50-155 TOL	ACTION NECESSARY <input type="checkbox"/>	CONCURRENCE <input type="checkbox"/>	DATE ANSWERED
DESCRIPTION: (Must Be Unclassified)		NO ACTION NECESSARY <input type="checkbox"/>	COMMENT <input type="checkbox"/>	BY:
Ltr trans the followings:	REFERRED TO	DATE	RECEIVED BY	DATE
	Fleury	6-1-67		
ENCLOSURES: (22 cys) (Notarized 5-26-67) Proposed <u>CHANGE # 13</u> , to Tech Specs requesting several changes.....w/incl. <u>Table- 1 & 2</u> <u>Figures- 1 thru 24</u> & (Fig. 25 also inserted) <u>References</u> Trans w/ ltr 5-29-67	Info cys to			
	Dr. Mann			
	Dr. Morris/Boyd			
	ubs/ Skovholt			
REMARKS:	Levine		DO NOT REMOVE	
DIST: 1- Formal 1- Suppl file 1- PDR 2- Compliance 1- OOC				